

**Bedrock geology Forsmark  
Modelling stage 2.3**

**Description of the bedrock geological  
map at the ground surface**

Michael B Stephens, Torbjörn Bergman  
Geological Survey of Sweden

Hans Isaksson, GeoVista AB

Jesper Petersson, SwedPower AB

December 2008

**Svensk Kärnbränslehantering AB**  
Swedish Nuclear Fuel  
and Waste Management Co  
Box 250, SE-101 24 Stockholm  
Phone +46 8 459 84 00



# **Bedrock geology Forsmark Modelling stage 2.3**

## **Description of the bedrock geological map at the ground surface**

Michael B Stephens, Torbjörn Bergman  
Geological Survey of Sweden

Hans Isaksson, GeoVista AB

Jesper Petersson, SwedPower AB

December 2008

This report concerns a study which was conducted for SKB. The conclusions and viewpoints presented in the report are those of the authors and do not necessarily coincide with those of the client.

A pdf version of this document can be downloaded from [www.skb.se](http://www.skb.se).

# Abstract

A description of the bedrock geological map of the ground surface at the Forsmark site is presented here. This map is essentially a 2D model for the distribution of different types of rock unit on this surface. Besides showing the distribution of these rock units, the bedrock geological map also displays the distribution of some deformation zones that intersect the ground surface. It also presents information bearing on the position and form of outcrops, the location and projection of boreholes drilled during the site investigation programme, subordinate rock types, the occurrence of abandoned mines or exploration prospects, measurements of ductile structures in outcrops, inferred form lines, key minerals, and the occurrence of mylonite and cataclastic rock.

Bedrock data from outcrops and excavations, airborne and ground magnetic data and information from the uppermost part of boreholes have all been used in the construction of the geological map. The description has also made use of complementary analytical data bearing on the composition and age of the rocks as well gamma-ray spectrometry and gravity data. Uncertainty in the position of the boundaries between rock units over the mapped area are addressed in a qualitative manner. Four model versions of the bedrock geological map have been delivered to SKB's GIS database (bedrock geological map, Forsmark, versions 1.1, 1.2, 2.2 and 2.3) at different times during the site investigation programme.

The Forsmark area is situated along the coast of the Baltic Sea in northern Uppland, Sweden, in a region where the overall level of ductile strain in the bedrock is high. This high-strain region extends several tens of kilometres across the WNW-ENE to NW-SE strike of the rocks in this part of the Fennoscandian Shield. At Forsmark, the coastal region is composed partly of high-strain belts, which formed under amphibolite-facies metamorphic conditions, and partly of tectonic lenses, where the bedrock is also affected by amphibolite-facies metamorphism but is affected, in general, by a lower degree of ductile strain and commonly folded. The ductile high-strain belts anastomose around the tectonic lenses. Regionally important, discrete deformation zones are situated within the broader, high-strain belts around the tectonic lenses and are retrograde in character. These include the Singö, Eckarfjärden and Forsmark zones.

Supracrustal rocks, here referred to as Group A, and three groups of meta-intrusive rocks, here referred to as Groups B, C and D, comprise the bedrock at Forsmark. These rock groups have been distinguished solely on the basis of their relative age relationships. The meta-intrusive rocks in Group B dominate. Two types of rock unit have been identified on the bedrock geological map of the area. These units distinguish areas composed of different dominant rock type or different style and intensity of ductile deformation.

The bedrock map has been divided into five separate subareas (subareas 1 to 5). These subareas trend in an approximately NW-SE direction and have been distinguished on the basis of the character of the ductile deformation in combination with the degree of homogeneity of the bedrock within each subarea. Contrasts between the different subareas are also visually prominent in the map of the total magnetic field. The lithologies, the character and orientation of ductile structures and the magnetic, gamma-ray spectrometry and gravity signatures are presented for each subarea.

# Contents

<b>1</b>	<b>Introduction</b>	7
1.1	Background	7
1.2	Objective, scope and contents	8
1.3	Regional geological setting	9
<b>2</b>	<b>Base data input and methodology</b>	11
<b>3</b>	<b>Complementary analytical data concerning the composition and age of rock types</b>	19
<b>4</b>	<b>Presentation of the bedrock geological map at the ground surface</b>	21
4.1	Geological components	21
4.1.1	Overview	21
4.1.2	Rock groups, mappable rock units and rock types	21
4.1.3	Subordinate rock types	23
4.1.4	Ductile structures and inferred form lines	23
4.2	Model versions	23
<b>5</b>	<b>Description of the bedrock geology at the ground surface</b>	29
5.1	Division into subareas	29
5.2	Description of subareas	29
5.2.1	Subarea 1 in the south-westernmost part of the mapped area	29
5.2.2	Subarea 2 in the south-western part of the mapped area	32
5.2.3	Subarea 3 in the central part of the mapped area including the candidate and target areas	38
5.2.4	Subarea 4 in the north-eastern part of the mapped area	43
5.2.5	Subarea 5 in the north-easternmost part of the mapped area	48
5.3	Summary	51
<b>6</b>	<b>Uncertainties</b>	53
<b>7</b>	<b>References</b>	55
<b>Appendix</b>	<b>Coding of rock type along cored boreholes drilled during the construction of the Forsmark nuclear power plant and SFR</b>	59

# 1 Introduction

## 1.1 Background

Since 2002, the Swedish Nuclear Fuel and Waste Management Company (SKB) has carried out investigations at two different locations, the Forsmark and Laxemar-Simpevarp areas, with the objective of siting a geological repository for spent nuclear fuel. The investigations have been conducted in campaigns separated by data freezes. After each data freeze, the site data have been analysed and modelling work has been completed. At Forsmark, data analysis and modelling work during the stage of investigations referred to as the initial site investigation resulted in two model versions (1.1 and 1.2). These models followed completion of model version 0 prior to the site investigation work. Modelling work during the subsequent complete site investigation has been carried out in three different stages (2.1, 2.2 and 2.3).

The candidate area at Forsmark (Figure 1-1) refers to the area at the ground surface that was recognised as suitable for a site investigation, following the feasibility study work /SKB 2000/. It extends from the Forsmark nuclear power plant in the north-west towards Kallrigafjärden in the south-east (Figure 1-1). The target area at Forsmark (Figure 1-1) was selected after the initial site investigation /SKB 2005a/ and formed the focus of activity during the complete site investigation work. It is situated in the north-western part of the candidate area, directly above the area at depth considered to be potentially suitable for the excavation of the waste repository at Forsmark.

At Forsmark, bedrock geological data from outcrops and helicopter airborne geophysical data were acquired during 2002 and 2003, with the primary aim to produce a 2D model for the distribution of different rock units at the ground surface, i.e. a bedrock geological map of the ground surface. This map has been of vital importance for the different versions and stages of the rock domain modelling work at the site and such modelling work has been of considerable significance for several other disciplines, including, for example, the development of thermal and rock mechanical models for the bedrock.

The bedrock geological map version 1.2 formed the keystone throughout the work at the site. It was presented in connection with completion of the initial site investigation /SKB 2005b/, after presentation of an earlier edition during model version 1.1 /SKB 2004/. This map was also used during model stage 2.1 /SKB 2006/. Minor adjustments to the bedrock geological map version 1.2 were carried out during the subsequent complete site investigation work and a modified version of the map was used in complementary modelling work during stages 2.2 and 2.3 /Stephens et al. 2007, 2008/. Minor adjustments have also been made in connection with the completion of this report.

The changes have taken account of the interpretation of high-precision ground magnetic data in the target area in the north-western part of the candidate area (Figure 1-1), and the results of both excavation and drilling activities. Since such changes were already foreseen at an early stage in the complete site investigation work, the detailed description of the bedrock geological map, originally planned to be completed in connection with model version 1.2, was postponed and moved forward to stage 2.3, following completion of all the site investigation work.

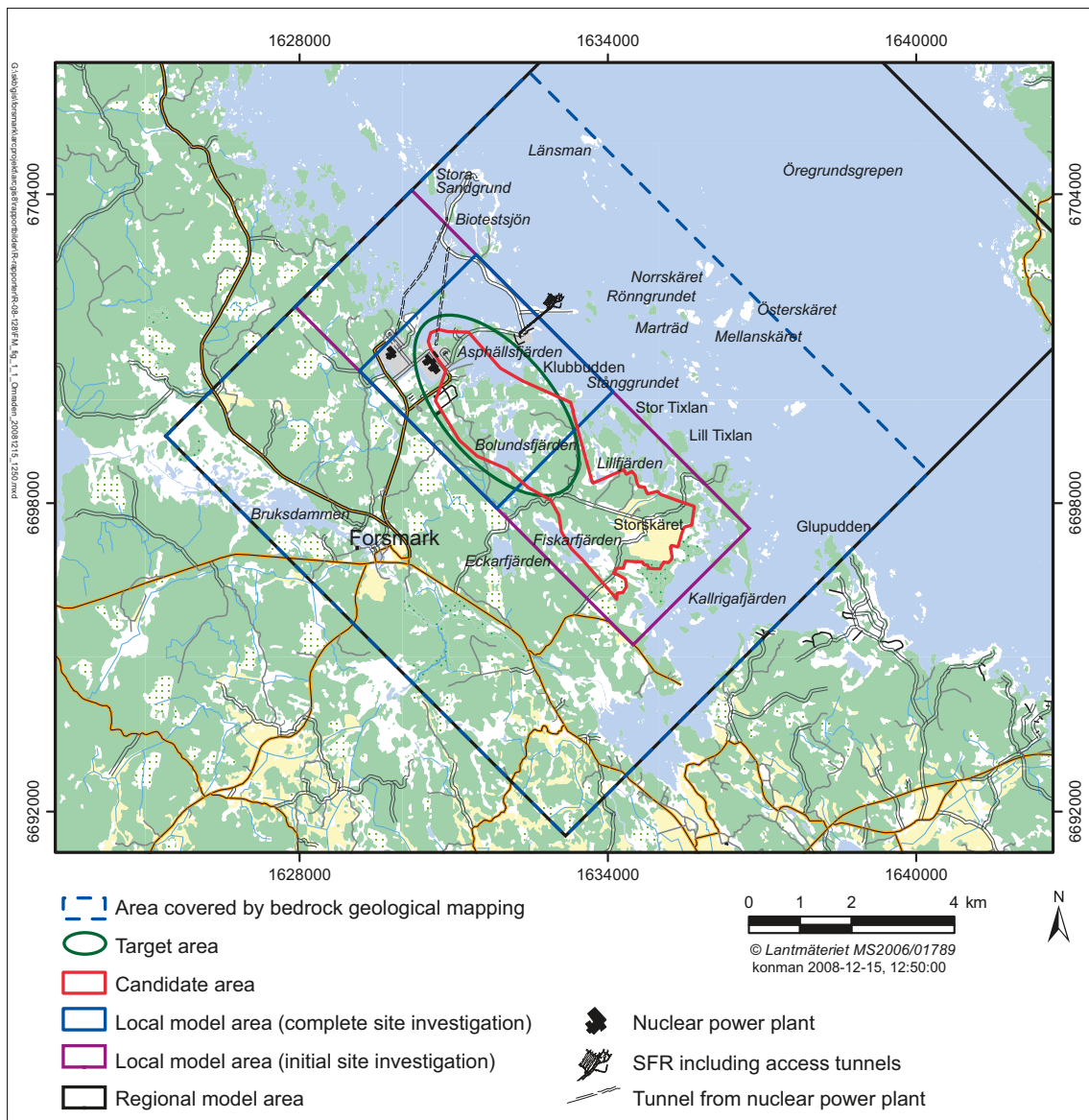


**Figure 1-1.** Area selected for bedrock geological mapping at Forsmark. All place names referred to in the text are also shown here.

## 1.2 Objective, scope and contents

This report aims to present a description of the bedrock geological map of the ground surface at Forsmark. This 2D model, which focuses attention on the distribution and character of different rock units at the surface, is confined to the area bounded by the coordinates (Easting/Northing) 1632471/6706371, 1640249/6698593, 1633178/6691522 and 1625400/6699300 in the RT 90, 2.5 gon W system.

The development of the bedrock geological map utilised relevant geological and geophysical data that exist within the map-area on land and in the archipelago close to Forsmark. Extrapolations over areas covered by water primarily made use of the geophysical data. A summary of these base input data and comments on the methodology used in the development of the geological map are provided in chapter 2.

Following each phase in the bedrock mapping work at the surface, complementary mineralogical, geochemical, petrophysical and geochronological data were acquired from both surface and drill core samples, and were subsequently evaluated. These data constrain more tightly, for example, the composition and age of the different rock types in each mappable rock unit. The results from these investigations have also been utilised in the description here. A compilation of the complementary data that bear on the composition and age of different rock types in the Forsmark area is provided in chapter 3.

A summary of the different geological components included in the GIS database (bedrock geological map) and the different model versions that have been developed during the site descriptive modelling programme at Forsmark is provided in chapter 4. The primary focus of the report is the description of the ground surface distribution and character of the mappable rock units within the area defined above. This description focuses particular attention on the lithology, the character of the ductile deformation and the geophysical signature within different subareas inside the mapped area, and is presented in chapter 5. Finally, comments on the uncertainties in the bedrock geological map are addressed in chapter 6.

### **1.3 Regional geological setting**

The Forsmark area is located along the coast of the Baltic Sea in northern Uppland within the municipality of Östhammar, approximately 120 km north of Stockholm (Figure 1-2). The area is situated in the south-western part of one of the Earth's ancient continental nuclei, referred to as the Fennoscandian Shield (Figure 1-2). This part of the shield belongs predominantly to the geological unit referred to as the Svecokarelian orogen (Figure 1-2). The bedrock inside the Earth's orogens was affected by major tectonic activity at a particular time interval during the Earth's long geological evolution and the actual geological process is referred to as orogeny. Tectonic activity refers to regional deformation and metamorphism of the crust in combination with active volcanism and the intrusion of igneous rocks at depth, i.e. major igneous activity. In essence, the branch of geology referred to as "tectonics" addresses the broad architecture of the outer part of the Earth.

The bedrock in the shield area around Forsmark formed between 1.9 and 1.85 billion years ago (1.9 to 1.85 Ga) and is dominated by different types of quartz-rich intrusive rocks (granitoids). The area consists of a flat topography with a dominance of till in the Quaternary overburden. The bedrock was affected by metamorphism under high-temperature conditions and by ductile deformation around and after 1.86 Ga, and by brittle deformation at several times after 1.8 to 1.7 Ga /SKB 2005b, Söderbäck (ed.) 2008/. The ductile deformation in the coastal region in northern Uppland gave rise to a relatively high concentration of large-scale high-strain belts and more spatially restricted zones oriented WNW-ESE to NW-SE. Tectonic lenses, in which the bedrock is much less affected by ductile deformation, are enclosed between the ductile high-strain belts. The candidate area is located in the north-westernmost part of one of these tectonic lenses that extends from north-west of the nuclear power plant in a south-eastward direction along the coast /SKB 2005b/. Subsequent brittle deformation in the candidate area has given rise to fracture zones that vary in size and frequency of occurrence. These zones are steeply dipping and oriented predominantly ENE-WNW to NNE-SSW or are gently dipping /Stephens et al. 2007/.

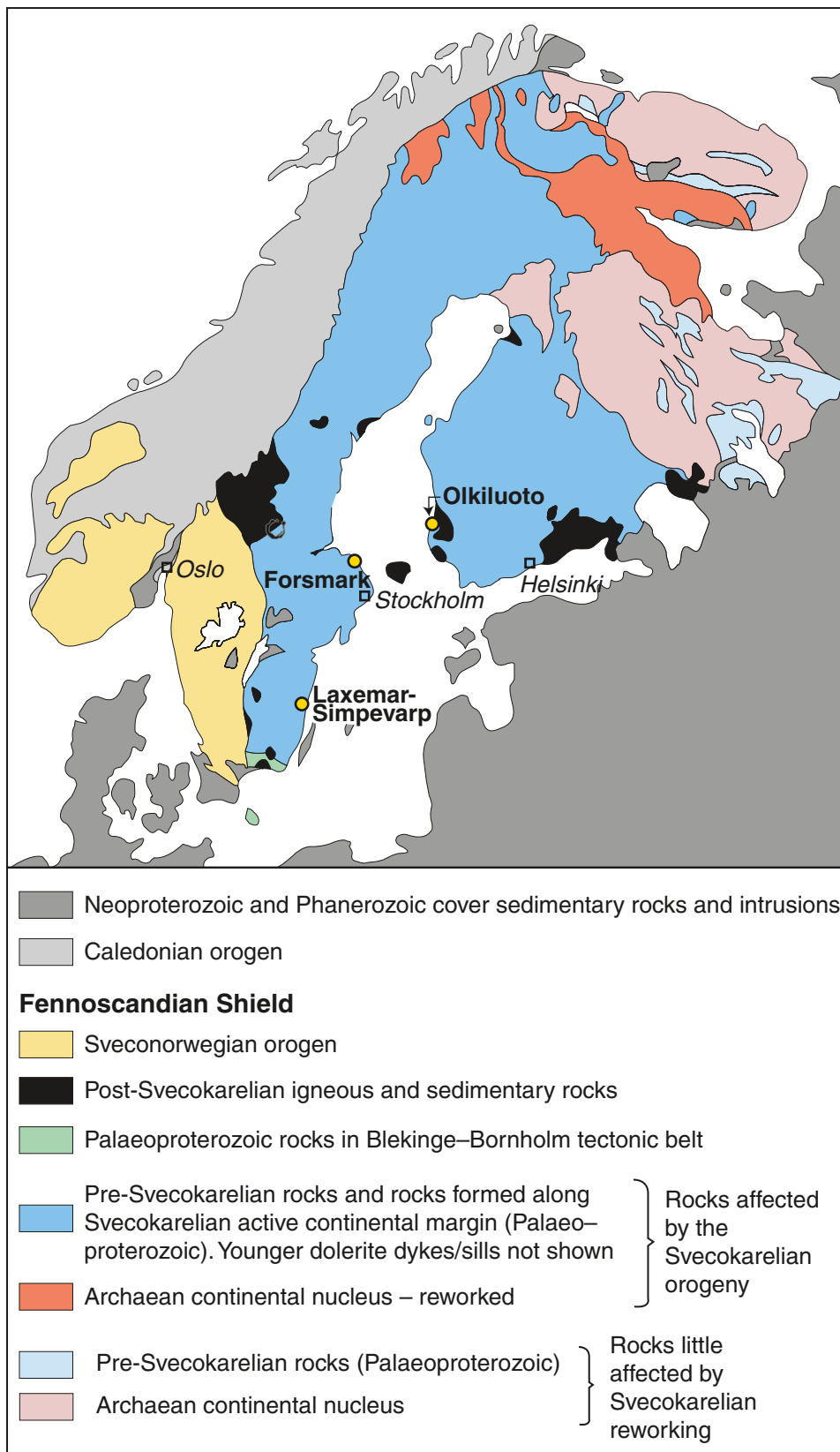


*Figure 1-2. Map showing the major tectonic units in the northern part of Europe at the current level of erosion (modified after /Koistinen et al. 2001/).*



## 2 Base data input and methodology

The following geological and geophysical information has been used in the compilation of the bedrock geological map over the Forsmark area:

- Outcrop data from 2,119 observation points on the mainland and in the archipelago area (Figure 2-1 and Figure 2-2) that were generated in connection with the bedrock mapping of the Forsmark site /Stephens et al. 2003a, Bergman et al. 2004/. The character of the bedrock on the mainland was also documented at the base of eight, temporarily exposed minor trenches and 21 shallow boreholes in the Quaternary cover /Bergman et al. 2004/.
- Detailed information on rock type at eight excavations (AFMxxxxxx on Figure 2-3) and in one large coastal outcrop (AFM001098 on Figure 2-3), where detailed mapping of fractures in the bedrock outside or across fracture zones has been carried out according to the SKB method description for detailed fracture mapping /Hermanson et al. 2003a, 2003b, 2004, Leijon (ed.) 2005, Cronquist et al. 2005, Forssberg et al. 2007, Petersson et al. 2007a/. Complementary detailed information on the character of fractures and rock type are also available from 44 smaller outcrops (Figure 2-3), which were investigated in connection with the bedrock mapping programme /Stephens et al. 2003a, 2003b/, and from excavations across two lineaments (Figure 2-3 and /Petersson et al. 2007b/).
- Rock type data from cored boreholes that were drilled in connection with the construction work at the nuclear power plant and at SFR, the repository for low- and intermediate-level radioactive waste, and along various shallow tunnels in the vicinity of these facilities. Most of these boreholes are also shallow (generally <50 m). These data provided constraints in areas that were either poorly exposed around the nuclear power plant or covered entirely by seawater. A summary of the work that converted information on rock types from these older cored boreholes into the rock nomenclature used in the Forsmark site investigation programme is presented in the appendix to this report.
- Rock type at the top of 25 telescope- or core-drilled boreholes and 38 percussion-drilled boreholes, which were completed during the site investigation programme at Forsmark. The locations of these boreholes are addressed later in chapter 4.
- Interpretation of the patterns on the magnetic anomaly map over the mainland and the archipelago area (Figure 2-4 and /Isaksson et al. 2004a/). This map is based primarily on helicopter airborne data acquired during 2002 /Rønning et al. 2003/. Fixed-wing airborne data from the Geological Survey of Sweden, acquired in connection with their standard geological mapping activities, were used in the easternmost and westernmost parts of the map-area where helicopter airborne data are lacking. The spatial resolution of the data from the Geological Survey of Sweden is four times lower than that obtained by the helicopter airborne measurements. Data input and the data processing used in the interpretation work are also presented in /Isaksson et al. 2004a/. This work was carried out independently of the evaluation of the outcrop data.
- Interpretation of the patterns on the magnetic anomaly map based on high-resolution ground magnetic data in the part of the map-area that corresponds to the target area (Figure 2-5 and /Isaksson et al. 2007/). The spatial resolution of these data is five times greater than that obtained by the helicopter airborne data.

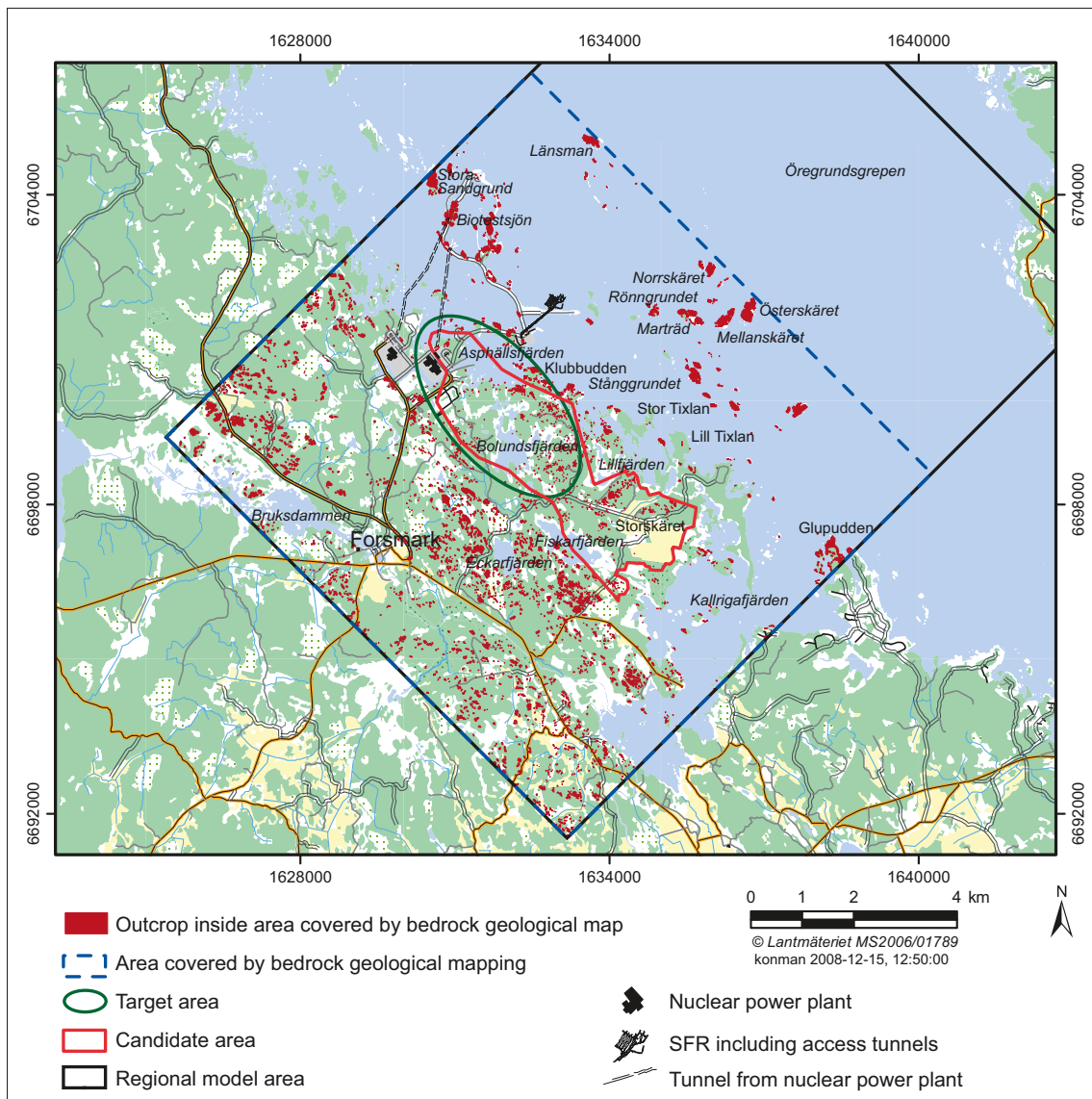


**Figure 2-1.** Position and form of outcrops in the area selected for bedrock geological mapping at Forsmark.

The development of the bedrock geological map on the mainland is based predominantly on the interpretation of the outcrop observations and, as a consequence, the quality of the map is strongly affected by outcrop frequency. The data from outcrop have been integrated with the interpretation of the airborne magnetic data in the 2D modelling work. The conclusions drawn from the interpretation of the magnetic data have played a subordinate role over a larger part of the mainland area. However, they are commonly of greater significance in the areas where the outcrop frequency is reduced. By contrast, in the archipelago area, the overall exposure of the bedrock is considerably lower and the interpretation of the magnetic data is of far greater significance. In the vicinity of the nuclear power plant and the SFR facility, where the helicopter airborne magnetic data are partly lacking or disturbed, the inspection of various reports and older cored boreholes (see also Appendix) aided the identification of rock units. Further comments on the uncertainty in the distribution of different rock units on the bedrock geological map are provided in chapter 6.

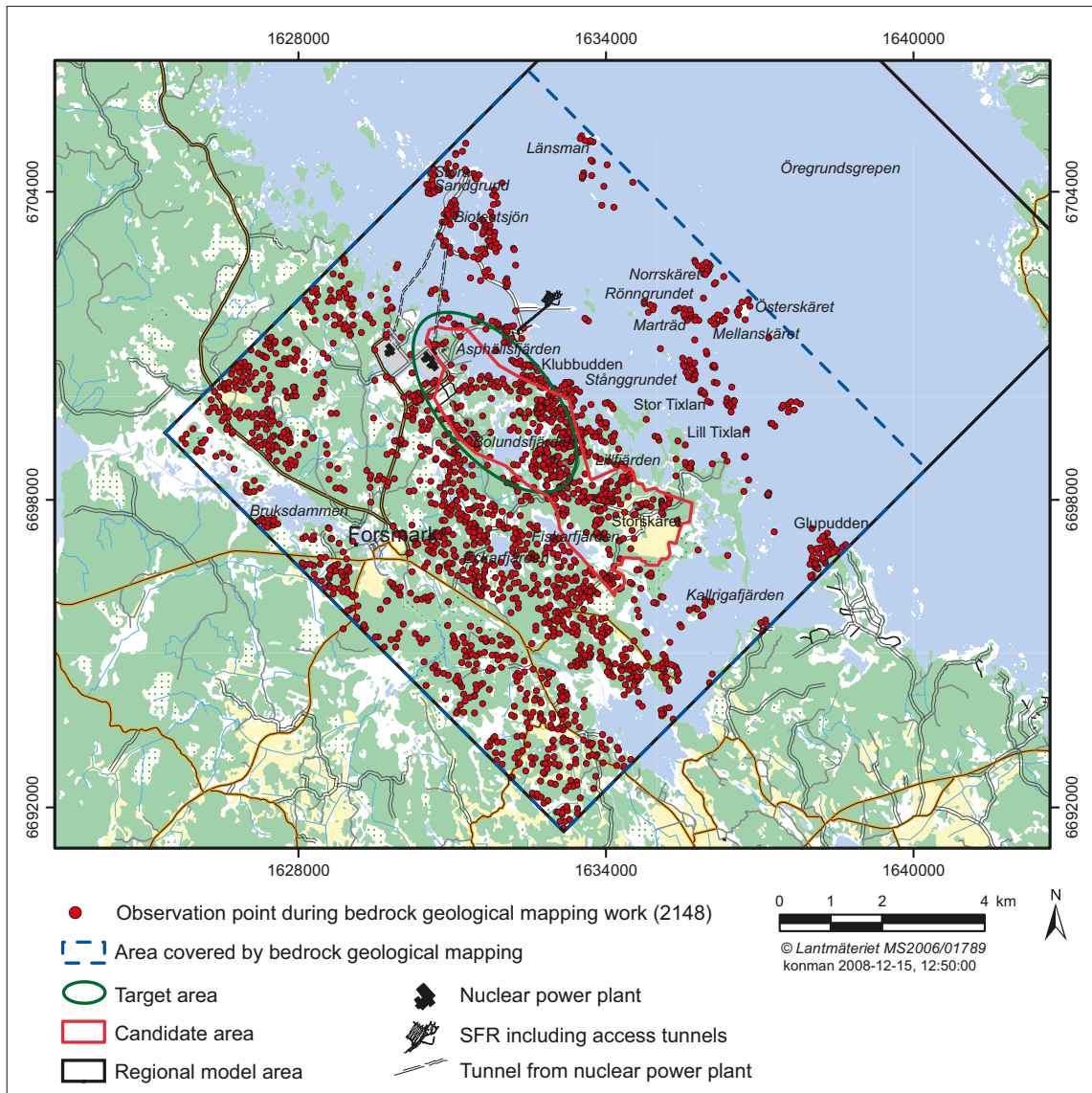


**Figure 2-2.** Observation points (PFMxxxxx) in the area selected for bedrock geological mapping at Forsmark /Stephens et al. 2003a, Bergman et al. 2004/.

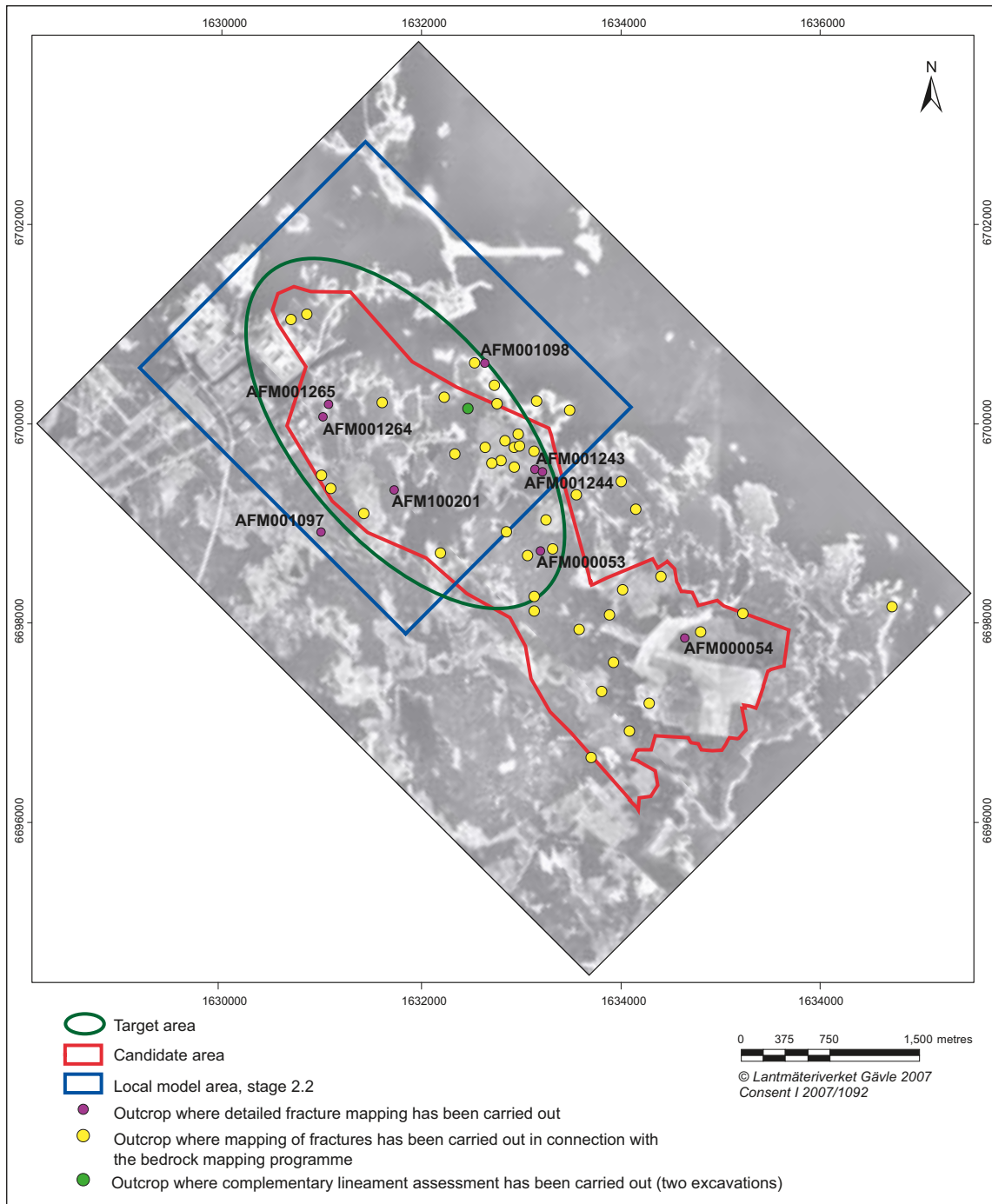


**Figure 2-3.** Location of outcrops and excavations where the mapping of fractures and rock types, and the complementary assessment of lineaments has been carried out.

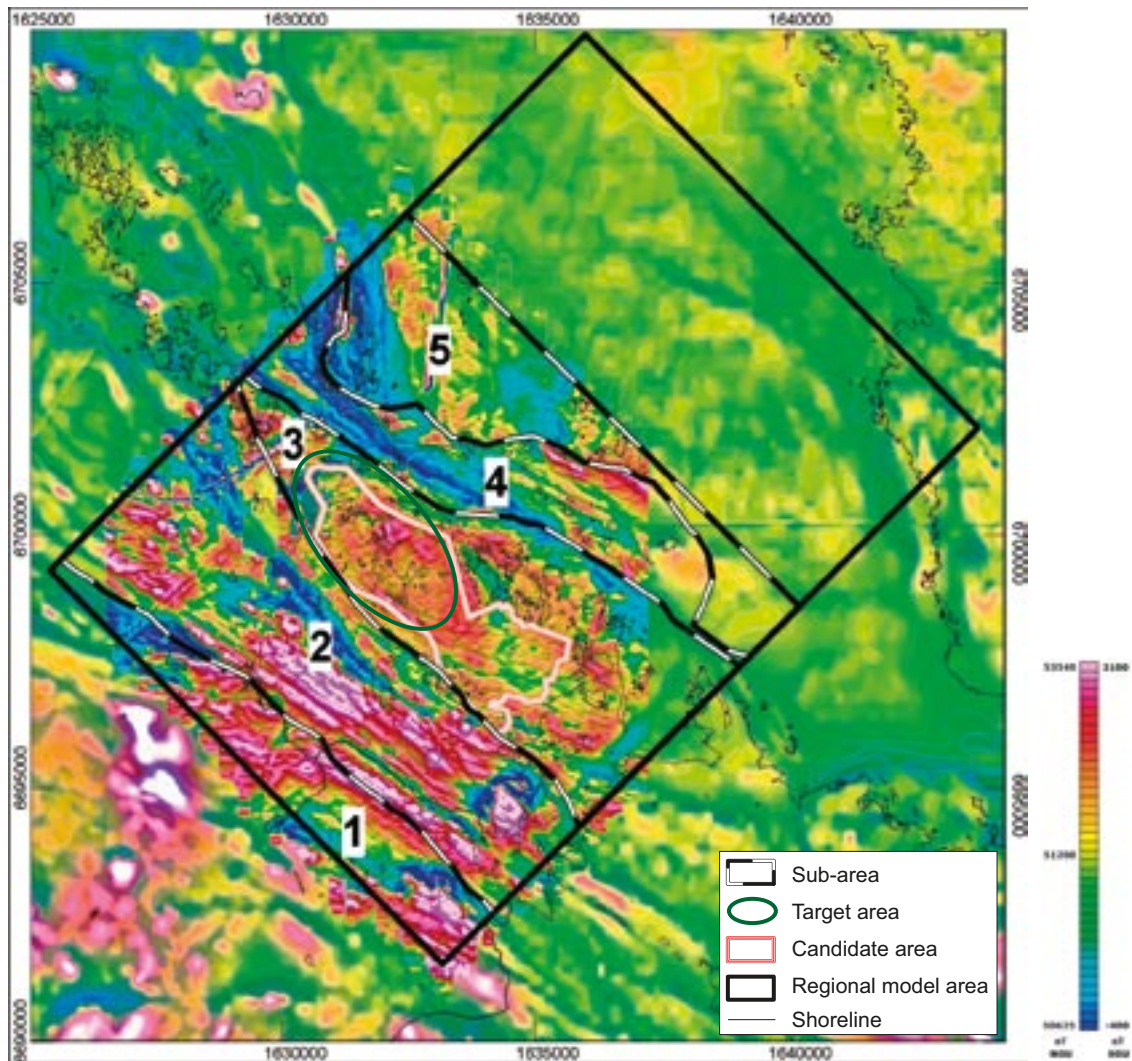


**Figure 2-4.** Map of the total magnetic field within and around the regional model area after /SKB 2005b/. In the major part of the area selected for bedrock geological mapping (subareas 1 to 5), helicopter airborne geophysical data are present and the map compilation shown here is based on data acquired in a north-south survey. In the remainder of and outside this area, the map of the total magnetic field is based on airborne data with lower spatial resolution provided by the Geological Survey of Sweden (SGU). Units in nanoTesla [nT]. Base level for the helicopter airborne survey (NGU) is 50,625 nT and for the standard airborne survey (SGU) -400 nT. The red-lilac end of the colour spectrum indicates more strongly magnetic bedrock and the blue end of the spectrum indicates more weakly magnetic bedrock. Helicopter data are lacking in the vicinity of the nuclear power plant (close to the number 3 on the map). The surveys are also disturbed by power lines and the Fenno-Scan HVDC (high voltage, direct current) cable in the area north-west of the power plant and in Öregrundsgrepen along coordinate grid line 1633000. The subareas outlined on the map (1–5) are defined and addressed in chapter 5. Further discussion of the different sets of magnetic data in the context of the modelling work is provided in /Stephens et al. 2007/, section 3.9.

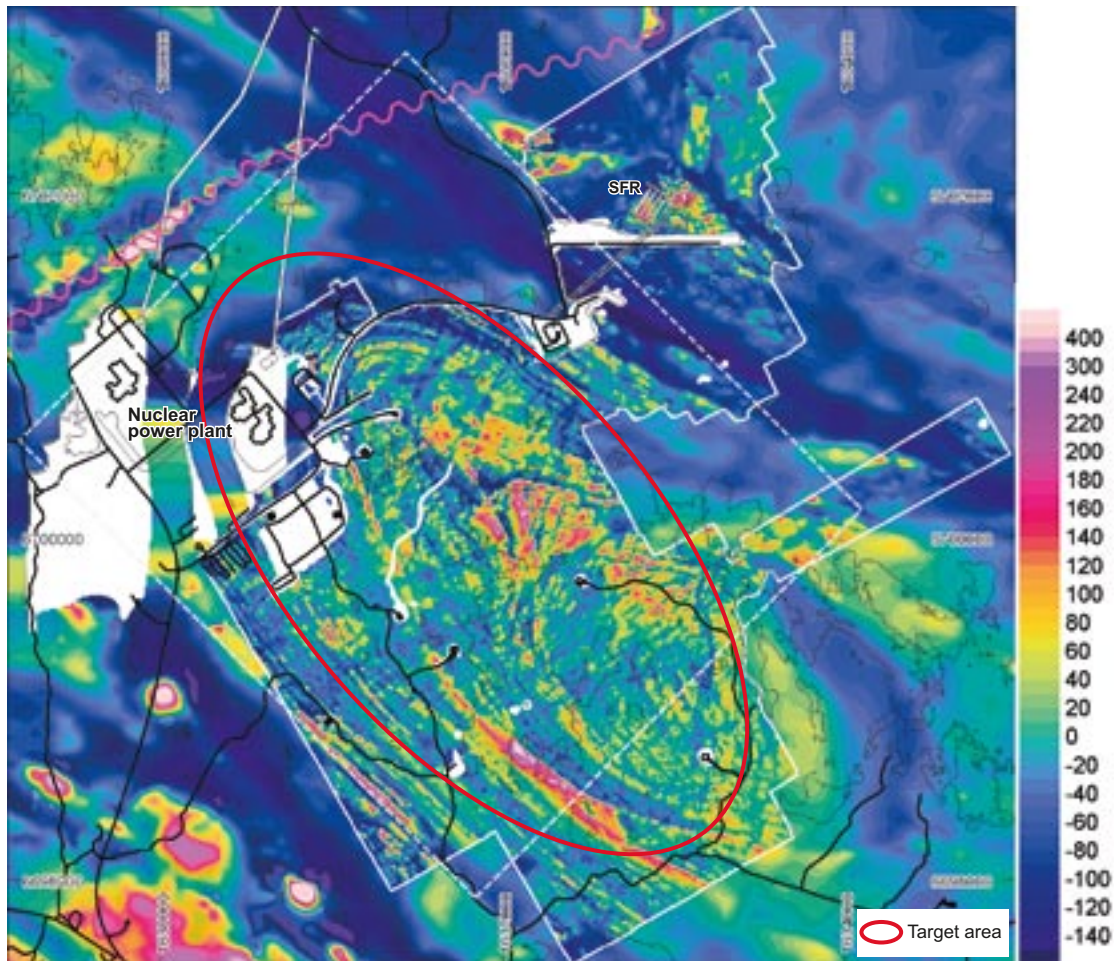


**Figure 2-5.** Map of the total magnetic field based on the north-south helicopter survey (see Figure 2-4) and the high-resolution ground magnetic survey (see overview in /Isaksson et al. 2007/). Units in nanoTesla [nT]. Base level for the helicopter borne survey is 51,230 nT and for the ground survey 51,407 nT. The local model area is outlined by a dashed white line and the detailed ground survey areas by a solid white line. White areas represent areas with poor coverage or poor quality due to disturbances. The magenta wavy line represents the location of the Fenno-Scan HVDC (high voltage, direct current) cable. Buildings, roads and drill sites in black. Tunnels and underground facilities at SFR are outlined by black lines and white filling. Further discussion of the different sets of magnetic data in the context of the modelling work is provided in /Stephens et al. 2007/, section 3.9.

The airborne geophysical measurements also generated various electromagnetic and gamma-ray spectrometry data /Rønning et al. 2003/ and the interpretation of these data were also addressed in /Isaksson et al. 2004a/. In particular, the gamma-ray spectrometry characteristics were described with the help of a classification scheme (Figure 2-6). However, data are lacking in the vicinity of the nuclear power plant and areas covered by water do not provide any information on the gamma-ray spectrometry. The interpretation of these complementary airborne geophysical data in the context of the evaluation of the outcrop data from the mapping work indicated that the former were of no help in the construction of the bedrock geological map. However, the classification scheme for the gamma-ray spectrometry data has been used here in the description of certain rock units (see chapter 5).

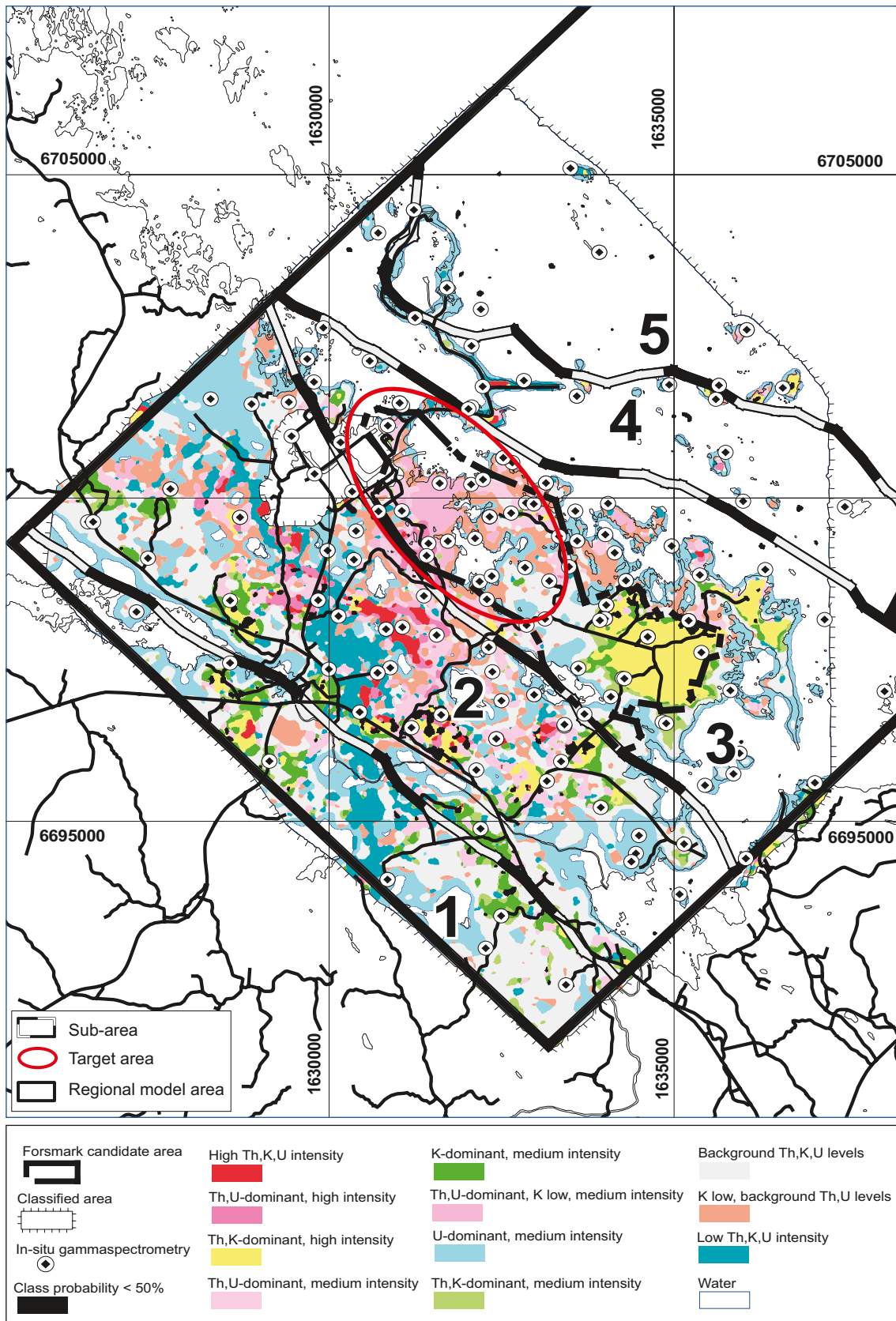


**Figure 2-6.** Classification of airborne gamma-ray spectrometry /Isaksson et al. 2004a/. Only data from the helicopter airborne geophysical survey are available. Data are lacking in the vicinity of the nuclear power plant. Areas covered by water do not provide any information on the gamma-ray spectrometry. The subareas outlined on the map (1–5) are defined and addressed in chapter 5.

Gravity data have also been acquired in the Forsmark area and a Bouguer gravity anomaly map has been constructed (Figure 2-7 and /Aaro 2003/). An evaluation of these data was completed during the complete site investigation stage after construction of the bedrock geological map version 1.2. For this reason, it was possible to utilise the gravity data as a test of the validity of the regional rock domain model for the site /Isaksson and Stephens 2007/, which, as indicated above, is strongly dependent on the quality of the bedrock geological map at the ground surface. As for the gamma-ray spectrometry data, the gravity data have only been used here in the description of certain rock units (see chapter 5).

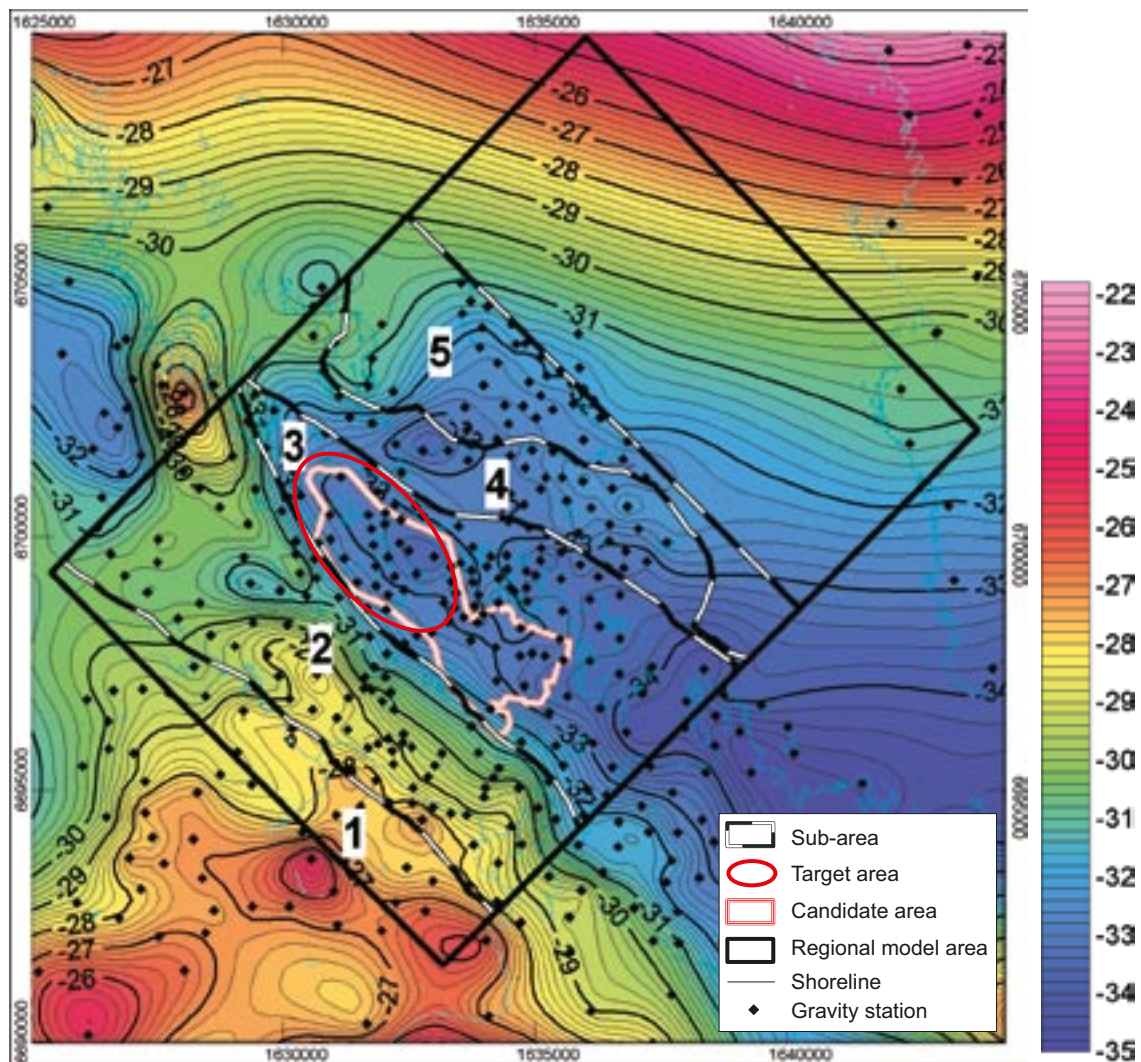


**Figure 2-7.** Bouguer gravity anomaly map (IGSN 71, equidistance 0.2 mgal) in the Forsmark area (modified after /Aaro 2003/). Units in milliGal (mGal). The subareas outlined on the map (1–5) are defined and addressed in chapter 5.



### 3 Complementary analytical data concerning the composition and age of rock types

The character of each rock type in an outcrop (e.g. composition, texture, type and orientation of ductile structures, magnetic susceptibility) has been documented during the bedrock mapping work /Stephens et al. 2003a, Bergman et al. 2004/. The composition was estimated solely by optical inspection. Complementary mineralogical, geochemical and petrophysical analyses of rock samples from both the ground surface and drill cores have been carried out, amongst other features, to constrain more tightly the composition of the different rock types, including altered rocks. The petrophysical analyses include silicate density data for the different rock types. The rock composition determined from the surface analytical data have been compared with that estimated in the field. In virtually all instances, the analytical data confirm the field estimates (see, for example, Stephens et al. 2003b, 2005 for the evaluation of the mineralogical and geochemical data). The description of the bedrock geological map in chapter 5 takes account of the more rigid assessment of the rock composition carried out in the complementary analytical data. For this reason, a compilation of the background reports that provide information on the complementary mineralogical, geochemical and petrophysical data is provided in Table 3-1.

Data bearing on the absolute age of different rock types have provided support to the recognition of different rock groups at Forsmark as inferred from the field relationships between the different lithologies (/Stephens et al. 2003b/ and chapter 4). The primary data reports are also listed in Table 3-1. An evaluation of these data in the context of the geological evolution in the Forsmark area is provided in /Söderbäck (ed.) 2008/.

**Table 3-1. List of SKB data reports where complementary information bearing on the composition and age of different rock types in the Forsmark area are presented.**

P-report	Reference
P-03-26	<b>Mattsson H, Isaksson H, Thunehed H, 2003.</b> Petrophysical rock sampling, measurements of petrophysical rock parameters and in situ gamma-ray spectrometry measurements on outcrops carried out 2002. Forsmark site investigation.
P-03-75	<b>Stephens M B, Lundqvist S, Bergman T, Anderson J, Ekström M, 2003.</b> Bedrock mapping. Rock types, their petrographic and geochemical characteristics, and a structural analysis of the bedrock based on Stage 1 (2002) surface data. Forsmark site investigation.
P-03-77	<b>Möller C, Snäll S, Stephens M B, 2003.</b> Dissolution of quartz, vug formation and new grain growth associated with post-metamorphic hydrothermal alteration in KFM02A. Forsmark site investigation.
P-03-102	<b>Isaksson H, Mattsson H, Thunehed H, Keisu M, 2004.</b> Interpretation of petrophysical surface data. Stage 1 (2002). Forsmark site investigation.
P-04-87	<b>Stephens M B, Lundqvist S, Bergman T, Ekström M, 2005.</b> Bedrock mapping. Petrographic and geochemical characteristics of rock types based on Stage 1 (2002) and Stage 2 (2003) surface data. Forsmark site investigation.
P-04-103	<b>Petersson J, Berglund J, Danielsson P, Wängnerud A, Tullborg E-L, Mattsson H, Thunehed H, Isaksson H, Lindroos, H, 2004.</b> Petrography, geochemistry, petrophysics and fracture mineralogy of boreholes KFM01A, KFM02A and KFM03A+B. Forsmark site investigation.
P-04-107	<b>Mattsson H, Thunehed H, Isaksson H, Kübler L, 2004.</b> Interpretation of petrophysical data from the cored boreholes KFM01A, KFM02A, KFM03A and KFM03B. Forsmark site investigation.
P-04-126	<b>Page L, Hermansson T, Söderlund P, Andersson J, Stephens M B, 2004.</b> Bedrock mapping U-Pb, <sup>40</sup> Ar/ <sup>39</sup> Ar and (U-Th)/He geochronology. Forsmark site investigation.
P-04-155	<b>Isaksson H, Mattsson H, Thunehed H, Keisu M, 2004.</b> Petrophysical surface data Stage 2 – 2003 (including 2002). Forsmark site investigation.
P-05-156	<b>Petersson J, Berglund J, Danielsson P, Skogsmo G, 2005.</b> Petrographic and geochemical characteristics of bedrock samples from boreholes KFM04A–06A, and a whitened alteration rock. Forsmark site investigation.

---

<b>P-report</b>	<b>Reference</b>
P-05-204	<b>Mattsson H, Thunehed H, Isaksson H, 2005.</b> Interpretation of petrophysical data from the cored boreholes KFM04A, KFM05A and KFM06A. Forsmark site investigation.
P-06-209	<b>Sandström B, Tullborg E-L, 2006.</b> Mineralogy, geochemistry, porosity and redox capacity of altered rock adjacent to fractures. Forsmark site investigation.
P-06-211	<b>Page L, Hermansson T, Söderlund P, Stephens M, 2007.</b> $^{40}\text{Ar}/^{39}\text{Ar}$ and U-Th/He geochronology: Phase II. Forsmark site investigation.

---

## **4 Presentation of the bedrock geological map at the ground surface**

### **4.1 Geological components**

#### **4.1.1 Overview**

The bedrock geological map at Forsmark (Figure 4-1 and Figure 4-2) is primarily a 2D model for the distribution of different rock units at the ground surface. Two types of rock unit have been identified and are displayed on the map. These rock units distinguish areas composed of different dominant rock type or different style and intensity of ductile deformation. Both rock units are described in more detail in section 4.1.2.

In general, bedrock geological maps also show the position and form of outcrops, the location and projection of boreholes, the distribution of deformation zones at the surface under investigation and, depending on the degree of detail required, various other base information that can be extracted from, for example, an outcrop database. At Forsmark, the deformation zones shown on different examples of the bedrock geological map reproduced in this report have been extracted from the stage 2.2 regional model for deformation zones at the site /Stephens et al. 2007/. Earlier versions of the map (see section 4.2) have used the information from earlier versions of the model for deformation zones. The following additional base information has been extracted from the outcrop database for Forsmark /Stephens et al. 2003a, Bergman et al. 2004/ and included in the map database as point or line information:

- Subordinate rock type.
- Ductile structures and inferred form lines.
- Abandoned mine or exploration prospect.
- Key mineral.
- Occurrence of mylonite and cataclastic rock.

In order to permit readability, the location of the point information on the map does not exactly correspond in space to the specific coordinates in the RT 90, 2.5 gon W system where the information was acquired. Furthermore, large areas on the map that lack such information generally correspond to areas where the bedrock is simply not exposed. For these two reasons, such point information needs to be handled carefully in any map inspection and most carefully in any statistical evaluation. The attributes “subordinate rock type” and “ductile structures and inferred form lines” are addressed in more detail in sections 4.1.3 and 4.1.4, respectively.

#### **4.1.2 Rock groups, mappable rock units and rock types**

The major groups of rocks in the Forsmark area (Groups A to D) are distinguished solely on the basis of their relative age relationships (/Stephens et al. 2003b/ and Table 4-1). One or more rock units, which are distinguished on the basis of the character of the dominant rock type, are included in each group (Table 4-1). Rock types within each rock unit are distinguished on the basis of their composition, grain size and relative age. A summary of the complementary data reports that provide base information on the mineralogical, geochemical and petrophysical character as well as the age of the different rock types named in Table 4-1 was provided in chapter 3.

**Table 4-1. Major rock groups and rock units at Forsmark based on /Stephens et al. 2003b, 2007/. The rock units in this table are distinguished on the basis of the character of the dominant rock type. SKB rock codes that distinguish different rock types within a rock unit are shown in brackets. The alteration code 104 for albitization is also included.**

Rock groups	Rock units on the bedrock geological map
<p>All rocks are affected by brittle deformation. The fractures generally cut the boundaries between the different rock types. The boundaries are predominantly not fractured.</p> <p>Rocks in Group D are affected only partly by ductile deformation and metamorphism.</p>	
Group D	<ul style="list-style-type: none"> <li>• Fine- to medium-grained granite and aplite (111058). Age partly 1.85 Ga.</li> <li>• Pegmatite, pegmatitic granite (101061).</li> </ul> <p>Variable age relationships with respect to Group C. Occur as dykes and minor bodies that are commonly discordant and, locally, strongly discordant to ductile deformation in older rocks.</p>
<p>Rocks in Group C are affected by penetrative ductile deformation under lower amphibolite-facies metamorphic conditions.</p>	
Group C	<ul style="list-style-type: none"> <li>• Fine- to medium-grained granodiorite, tonalite and subordinate granite (101051). Age 1.86 Ga.</li> </ul> <p>Occur as lenses and dykes in Groups A and B. Intruded after some ductile deformation in the rocks belonging to Groups A and B with weakly discordant contacts to ductile deformation in these older rocks.</p>
<p>Rocks in Groups A and B are affected by penetrative ductile deformation under amphibolite-facies metamorphic conditions and are locally migmatitic.</p>	
Group B	<ul style="list-style-type: none"> <li>• Biotite-bearing granite (101057) and aplitic granite (101058), both with amphibolite (102017) as dykes and irregular inclusions. Local albitization (104) of granitic rocks. Age 1.87 to 1.86 Ga.</li> <li>• Granodiorite (101056).</li> <li>• Tonalite to granodiorite (101054) with amphibolite (102017) enclaves. Age 1.88 Ga.</li> <li>• Diorite, quartz diorite and gabbro (101033). Age 1.89 Ga.</li> <li>• Ultramafic rock (101004).</li> </ul>
Group A	<ul style="list-style-type: none"> <li>• Sulphide mineralisation, possibly epigenetic (109010).</li> <li>• Calc-silicate rock (108019), iron oxide mineralisation (109014).</li> <li>• Felsic to intermediate volcanic rock (103076). Age 1.89 Ga or older.</li> <li>• Sedimentary rock (106001). Age 1.89 Ga or older.</li> </ul>

The bedrock geological map at Forsmark also distinguishes rock units where the rocks are banded and/or affected by a strong, ductile tectonic foliation (black dots in Figure 4-1 and Figure 4-2) from units where the rocks are folded and more lineated in character (black dots absent in Figure 4-1 and Figure 4-2). The former are inferred to be affected by higher ductile strain and anastomose around the more folded and lineated bedrock with lower ductile strain inside several tectonic lenses. In the Forsmark area, the units affected by higher ductile strain commonly correspond to more heterogeneous bedrock. The candidate area is situated inside one of the tectonic lenses and includes the target area in its north-western part, between Lake Bolundsfjärden and the nuclear power plant (Figure 4-1 and Figure 4-2). This lens is referred to as the Forsmark tectonic lens.

### 4.1.3 Subordinate rock types

Subordinate rock types observed at an outcrop are illustrated on the map with the help of point information. These rocks occur as:

- Xenoliths of predominantly Group A supracrustal rocks within younger, intrusive rocks.
- Amphibolite enclaves in metatonalite (Group B).
- Amphibolite dykes and irregular inclusions in biotite-bearing metagranite and aplitic metagranite (Group B).
- Bands and lenses of one rock type within another. The bands and lenses may be deformed dykes, deformed inclusions or both these possibilities.
- Dykes and minor intrusions of rocks that belong to the younger Group C and Group D rock groups.

The amphibolite enclaves, dykes and irregular inclusions, and the various bands and lenses generally trend parallel or sub-parallel to the tectonic foliation, whereas the younger Group C and Group D rocks display a more varied orientation. This feature is addressed in more detail in the description of the bedrock geological map that is presented in section 5.

### 4.1.4 Ductile structures and inferred form lines

Ductile planar structures at the Forsmark site consist of a tectonic foliation, a tectonic banding or a combined foliation and banding. These structures vary considerably in their degree of development and this variation is interpreted to reflect a variation in the degree of ductile deformation over the area (see below). The foliation corresponds to a planar grain-shape fabric. In the dominant felsic rocks that belong to Groups A and B (Table 4-1), this fabric is defined by oriented grains of biotite and, less commonly, hornblende, as well as elongate aggregates of recrystallised quartz and feldspar.

A ductile linear structure that corresponds to a linear grain-shape fabric is conspicuous over the whole area. This mineral lineation is inferred to mark the direction of stretching during the ductile deformation. Oriented hornblende crystals in the Group B mafic and intermediate rocks define this fabric most conspicuously. Oriented biotite grains and elongate aggregates of recrystallised quartz and feldspar also form the lineation in the felsic rocks that belong to Groups A, B and C. Minor folds that deform the foliation or tectonic banding define a second type of ductile linear structure.

In order to provide some insight into the trace of regional ductile structures at the ground surface, inferred form lines for the two structural components tectonic banding and tectonic foliation have been constructed and included in the map database.

## 4.2 Model versions

The first version of the bedrock geological map, which covered essentially the major part of the land area at Forsmark, was presented in connection with the preliminary site descriptive model version 1.1 (Figure 4-9 in /SKB 2004/). This map made use of the outcrop data generated during the first stage of the geological mapping of the bedrock during 2002 and the acquisition of helicopter airborne geophysical data. The bedrock geological map covered the area bounded by the coast to Öregrundsgrepen in the north-east, Kallrigafjärden in the south-east, the north-western boundary to the regional model area in the north-west (Figure 1-1) and the Forsmark deformation zone in the south-west. The geological map presented in connection with the completion of the initial site investigations and the preliminary site description version 1.2 (Figure 5-12 in /SKB 2005b/) has formed the keystone throughout the work at the site. This map was compiled after completion of all the bedrock mapping work at the surface during 2003.

Minor adjustments to the bedrock geological map have been completed during the modelling work in connection with the complete site investigations. The acquisition of high-resolution ground magnetic data in the target area and the interpretation of magnetic minima connections resulted in necessary changes to the boundaries of rock units in the poorly exposed area around the eastern part of Asphällsfjärden, close to the peninsula referred to as Klubbudden (Figure 4-1). These revisions were described during model stage 2.2 (cf. Figures 3-3 and 3-4 in /Stephens et al. 2007/). Finally, very minor adjustments to the boundaries between some rock units on the basis of, for example, the drilling of boreholes HFM30 and KFM11A were completed outside the candidate area during model stage 2.3. Four model versions of the bedrock geological map have been delivered to SKB's GIS database (bedrock geological map, Forsmark, versions 1.1, 1.2, 2.2 and 2.3).

The stage 2.3 bedrock map that covers the whole area selected for geological mapping is shown in Figure 4-1. This image only shows the surface distribution of different rock units, the surface distribution of regional deformation zones with a trace length at the ground surface greater than 10,000 m, abandoned mines or exploration prospects and the location and projection of boreholes drilled during the site investigation programme. For purposes of clarity, other attributes are omitted.

The bedrock map that places focus on the target area to the south-east of the nuclear power plant is presented in Figure 4-2. This map shows the surface distribution of different rock units, the surface distribution of all the deformation zones included in the regional model stage 2.2 (i.e. steeply dipping deformation zones with a trace length at the ground surface greater than 3,000 m and gently dipping fracture zones), information bearing on the position and form of outcrops, the location and projection of boreholes drilled during the site investigation programme, subordinate rock types, measurements of ductile structures in outcrops, inferred form lines, key minerals, and the occurrence of mylonite and cataclastic rock. There are no abandoned mines or exploration prospects in the area shown in Figure 4-2.

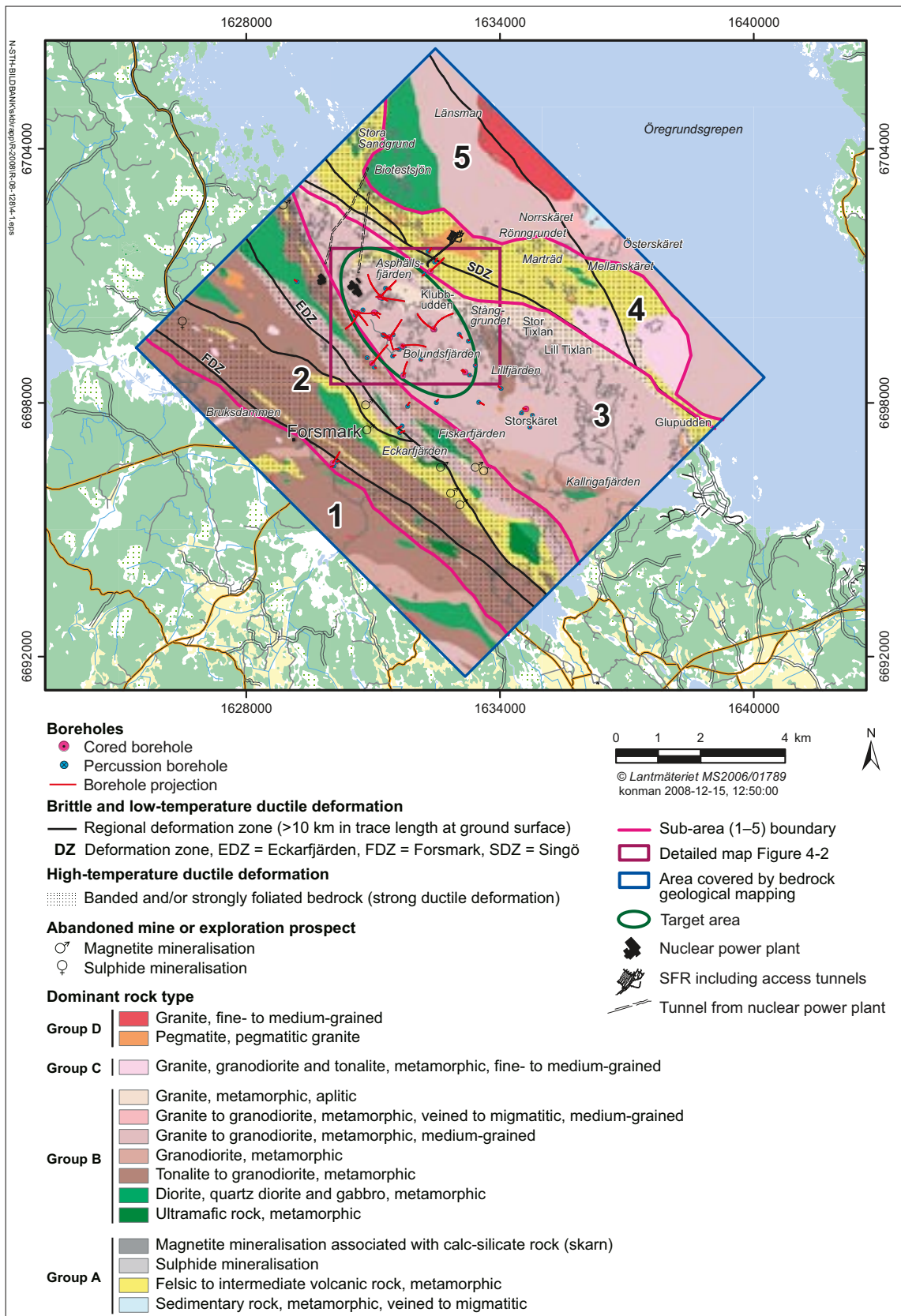


**Figure 4-1.** Simplified bedrock geological map of the Forsmark area. Deformation zones with a trace length at the ground surface greater than 10,000 m, abandoned mines or exploration prospects and boreholes drilled during the site investigation programme are also shown on the map. The location of the deformation zones is based on the regional deformation zone model, stage 2.2. For purposes of clarity, other geological features are not shown on the map. The subareas outlined on the map (1–5) are defined and addressed in chapter 5. Coordinates are provided using the RT 90, 2.5 gon W system.

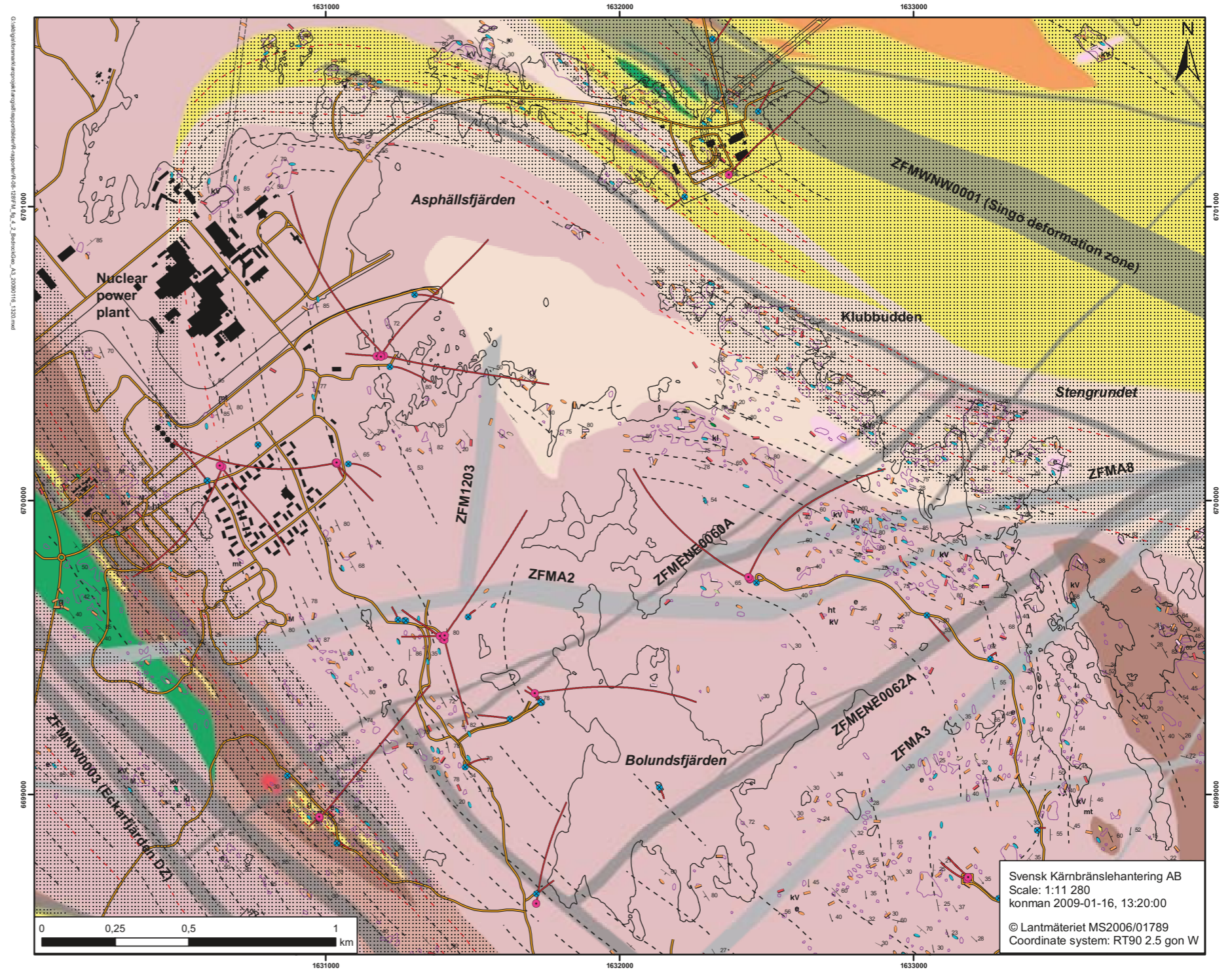


**Figure 4-2.** Detailed bedrock geological map of the target area and its immediate surroundings at Forsmark. Gently dipping fracture zones and steeply dipping deformation zones with a trace length at the ground surface greater than 3,000 m are shown on the map. The location of these zones at the ground surface is based on the regional deformation zone model, stage 2.2. Outcrops, boreholes drilled during the site investigation programme, subordinate rock types, measurements of ductile structures, inferred form lines, key minerals, and the occurrence of mylonite and cataclastic rock are also shown on the map. Coordinates are provided using the RT 90, 2.5 gon W system.



## **5 Description of the bedrock geology at the ground surface**

### **5.1 Division into subareas**

The bedrock geological map can be divided into five subareas that trend in an approximately NW-SE direction (Figure 4-1). These subareas have been distinguished on the basis of the general character of the ductile deformation in combination with the degree of homogeneity of the bedrock, as revealed during the geological mapping work. Contrasts between the different subareas are also visually prominent in the map of the total magnetic field (Figure 2-4). These features are addressed in detail for each subarea in the description below.

### **5.2 Description of subareas**

#### **5.2.1 Subarea 1 in the south-westernmost part of the mapped area**

##### ***Lithology***

The bedrock in the south-westernmost part of the mapped area (subarea 1 in Figure 4-1) is dominated by grey to reddish grey, medium-grained metatonalite or metagranodiorite (Figure 4-1 and Figure 5-1a). Inclusions or dyke-like bodies of amphibolite (Figure 5-1b) form a conspicuous, subordinate rock type. The metatonalites and metagranodiorites are predominantly equigranular. However, immediately south of the Forsmark village, rocks with a granodioritic composition show a porphyritic texture with larger crystals of K-feldspar (Figure 5-1c). Metagranite, similar to that observed in the candidate area (see subarea 3 below), is present in the southernmost part of the mapped area (Figure 4-1). All these rocks belong to the Group B intrusive suite that has been recognized in the Forsmark area (/Stephens et al. 2003b/ and Table 4-1).

Several minor bodies of metagabbro, metadiorite, quartz-bearing metadiorite and, locally, even dark ultramafic rock, also included in the Group B intrusive suite, are conspicuous in the subarea (Figure 4-1). These rocks are occasionally intruded by a network of dykes with a granitic composition (Figure 5-1d). South-west of the Forsmark village, a strongly banded sequence of fine-grained metavolcanic rock with a dacitic to andesitic composition (Group A), amphibolite and calc-silicate rock is also present (Figure 4-1). All these occurrences have been marked on the geological map with a lens-like form within the dominant metatonalite or metagranodiorite.

Two types of younger, minor intrusive rocks form subordinate rock units in the subarea (Figure 4-1). These include grey to reddish grey, fine- to medium-grained metagranodiorite or metatonalite (Group C) and fine- to medium-grained, pale red metagranite (Group D). Dykes, segregations and minor bodies of pegmatite and pegmatitic granite (Group D) are common at outcrop scale, but do not form any mappable rock unit inside the subarea.

##### ***Ductile structures***

In general, the bedrock in the south-westernmost part of the mapped area is compositionally more homogeneous and affected by a lower degree of ductile strain relative to the rocks in subarea 2 immediately to the north-east. A linear grain-shape fabric is the dominant ductile structure in the bedrock in subarea 1 (Figure 5-1a). In a structural sense, the bedrock is predominantly composed of LS-tectonites. A more intense planar fabric with the occurrence of a tectonic banding is present in the metavolcanic rocks south-west of the Forsmark village and these have been designated as a rock unit affected by higher ductile strain on the geological map (Figure 5-2).

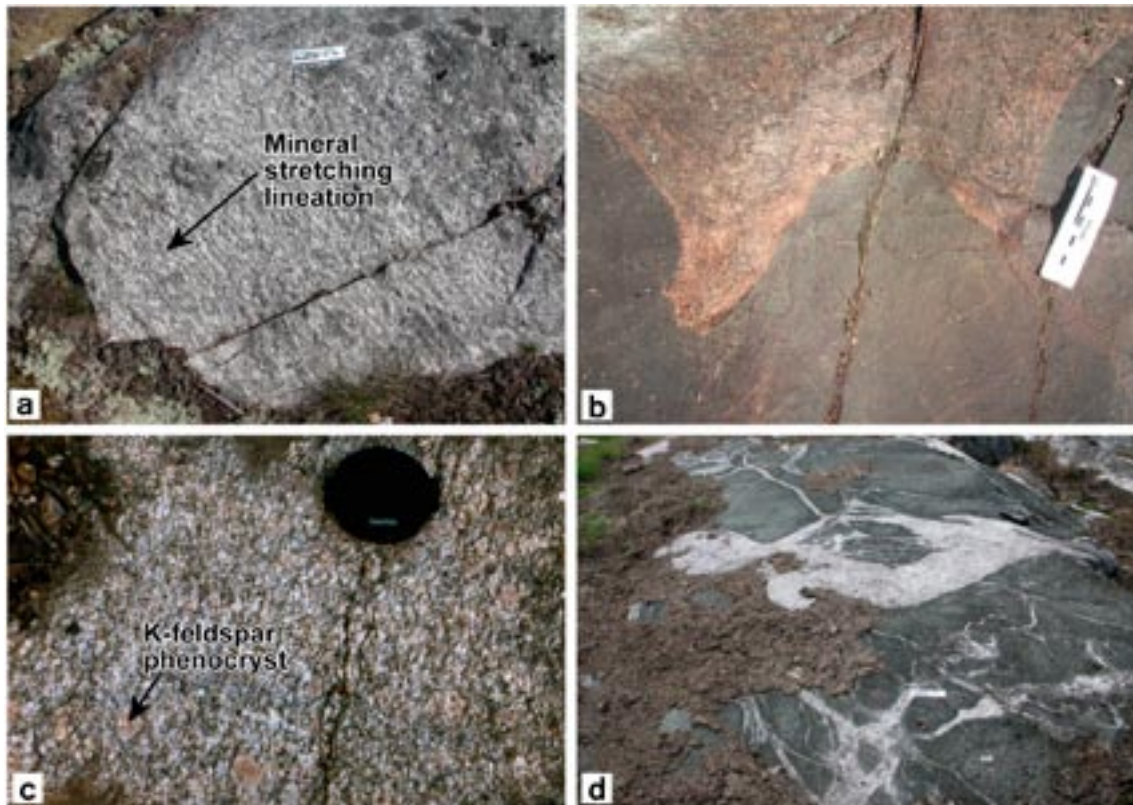


**Figure 5-1.** Field character of the rocks inside subarea 1 in the south-westernmost part of the area selected for mapping at Forsmark. a) Mineral stretching lineation in Group B metatonalite (observation point PFM000591). b) Group B metagranodiorite in contact with amphibolite. The metagranodiorite is strongly foliated close to the contact with the amphibolite (PFM000937). c) Group B porphyritic metagranodiorite with K-feldspar phenocrysts (PFM005174). d) Group B ultramafic rock injected by a network of pegmatitic granite (PFM000590).

Both the mineral stretching lineation and the fold axes in the subarea plunge moderately to the south-east and the planar structures dip steeply to the south-west (Figure 5-2). The amphibolites in the subarea are oriented more or less parallel to the tectonic foliation or banding in the bedrock (Figure 5-2). By contrast, the younger granitic and pegmatitic dykes (Group D) show a more variable orientation (Figure 5-2).

### **Geophysical signature**

The south-westernmost part of the mapped area in subarea 1 is characterised by a banded magnetic anomaly pattern with medium to high intensity (Figure 2-4 and /Isaksson et al. 2004a/). In general, the magnetic connections trend WNW-ESE but, in the vicinity of subarea 2, the trend is closer to NW-SE and the banded pattern is more intense (Figure 2-4). Inspection of the airborne magnetic map over a larger area (see, for example, /Bergman et al. 1999/) suggests that the subarea is situated on the north-eastern flank of a major fold structure with an axial surface trace that trends NW-SE. In the south-eastern part of subarea 1, an intrusion with gabbroic composition correlates with a strong, semi-circular magnetic anomaly with an irregular pattern (Figure 2-4).

The airborne gamma-ray spectrometry map generally shows background potassium, uranium and thorium levels with only limited areas of higher intensity (Figure 2-6 and /Isaksson et al. 2004a/). In the central part of the subarea, a uranium dominant area that trends north-south with enhanced intensity could not be verified in the field and the anomaly can be related to levelling problems along parts of the corresponding airborne survey lines.

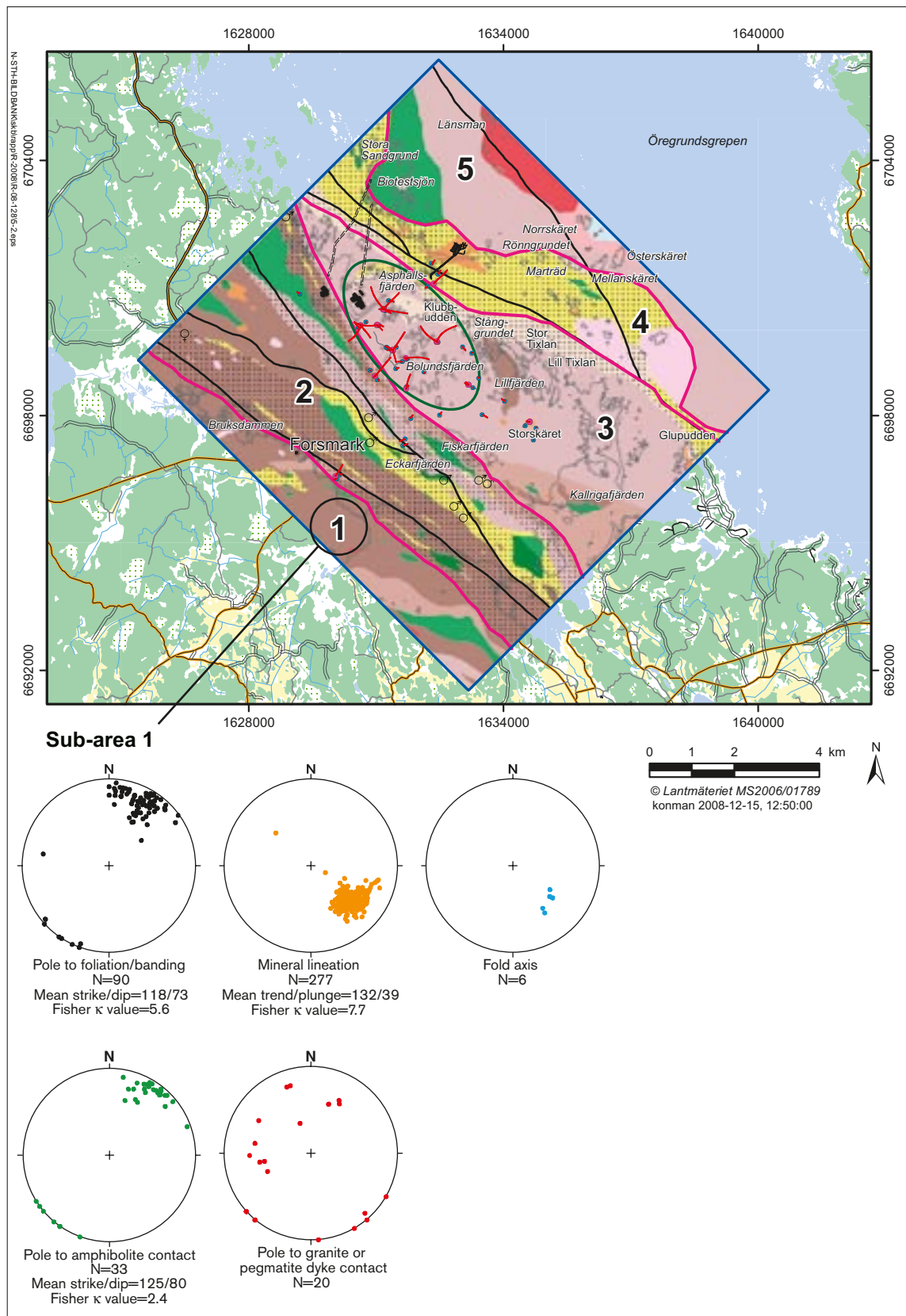


**Figure 5-2.** Orientation of ductile structures, amphibolites and Group D granitic and pegmatitic dykes at the ground surface in subarea 1. All structures and rock contacts have been plotted on the lower hemisphere of a Schmidt, equal-area stereographic projection. Planar structures and rock contacts have been plotted as poles to planes. The stereographic projections for the ductile structures are taken from /Stephens et al. 2003b/. The base map is the bedrock geological map of the area (see Figure 4-1 for legend).

The Bouguer anomaly map (Figure 2-7) shows that the subarea in the south-westernmost part of the mapped area is located south-west of a steep gradient in the gravity field, which is oriented in a NW-SE direction. Furthermore, it constitutes the north-eastern boundary of a high gravity plateau to the south-west. This plateau region is dominated by rocks with tonalitic and granodioritic composition and, locally, dioritic, gabbroic and ultramafic rocks /Stålhös 1991/. The rocks with intermediate to ultramafic composition are the source of restricted high gravity anomalies that indicate a distinctive mass excess.

## 5.2.2 Subarea 2 in the south-western part of the mapped area

### *Lithology*

The bedrock in the area between the southern part of Kallrigafjärden in the south-east and north of Forsmark village in the north-west contains several different rock units (subarea 2 in Figure 4-1). Rock units dominated by metatonalite or metagranodiorite and with subordinate amphibolite, similar to that observed in the south-westernmost part of the mapped area, are most conspicuous (Figure 5-3a and Figure 5-3b). A minor sulphide mineralisation is hosted by metagranodiorite in the north-western part of the subarea (Björnbo, PFM000454, 6699831/1626493). A rock unit composed of pale red, strongly foliated metagranite, which is predominantly medium-grained but also aplitic in character, has been mapped in a NW-SE strike direction from Kallrigafjärden via Eckarfjärden to the area south-west of the nuclear power plant. This unit more or less follows the regionally significant Eckarfjärden deformation zone (see below). All these intrusive rocks belong to the Group B intrusive rock suite (/Stephens et al. 2003b/ and Table 4-1).

Several mappable units of felsic to intermediate metavolcanic rock (Group A) are present in the subarea, the thickest unit extending in a NW-SE strike direction from Kallrigafjärden to north-west of Eckarfjärden (Figure 4-1). The bedrock in these units is commonly banded, with a dominant component that consists of grey to dark grey, fine-grained, felsic to intermediate rock and subordinate amphibolite. The former is predominantly dacitic to andesitic in composition /Stephens et al. 2003b, 2005/ and shows a banding defined by paler, more quartz- and feldspar-rich layers that alternate with layers richer in biotite (Figure 5-3c), locally with garnet. Due to the effects of ductile deformation and recrystallisation under amphibolite-facies metamorphic conditions, considerable uncertainty remains concerning to what extent the banded rocks represent syn-eruptive, resedimented, volcanoclastic rocks or even post-eruptive, volcanogenic sedimentary rocks /Stephens et al. 2003b/. There is also uncertainty in the origin of the more homogeneous rocks which may represent pyroclastic deposits, lavas or synvolcanic intrusive rocks /Stephens et al. 2003b/.

The metavolcanic units host several magnetite mineralisations (Figure 4-1). These mineralisations are commonly impregnated with sulphides and are spatially associated with amphibole-garnet calc-silicate rock (skarn). Several mineralisations (e.g. Skomakargruva, PFM000446, 6697966/1630821) have been the focus of exploration and mining activity in historical time. Pyroxene-epidote calc-silicate rock (skarn), without magnetite mineralisation, also occurs as thin, up to metre-thick sheets in the felsic metavolcanic rocks.

An assessment of the potential of the Forsmark area for exploration after metallic and industrial mineral deposits has been presented in /Lindroos et al. 2004/. A potential for iron oxide mineralisation and possibly base metals was recognised. A mineral resource map (Figure 5-4) shows how the areas that bear this potential are concentrated in subarea 2 in the south-western part of the mapped area, predominantly in the felsic to intermediate metavolcanic rocks. Geochemical analyses of till at Forsmark provide support to this conclusion /Nilsson 2003/. However, the minor iron mineralisations in the Forsmark area have been judged to have no economic value and this judgement is also deemed to be valid in the long-term perspective /Lindroos et al. 2004/.

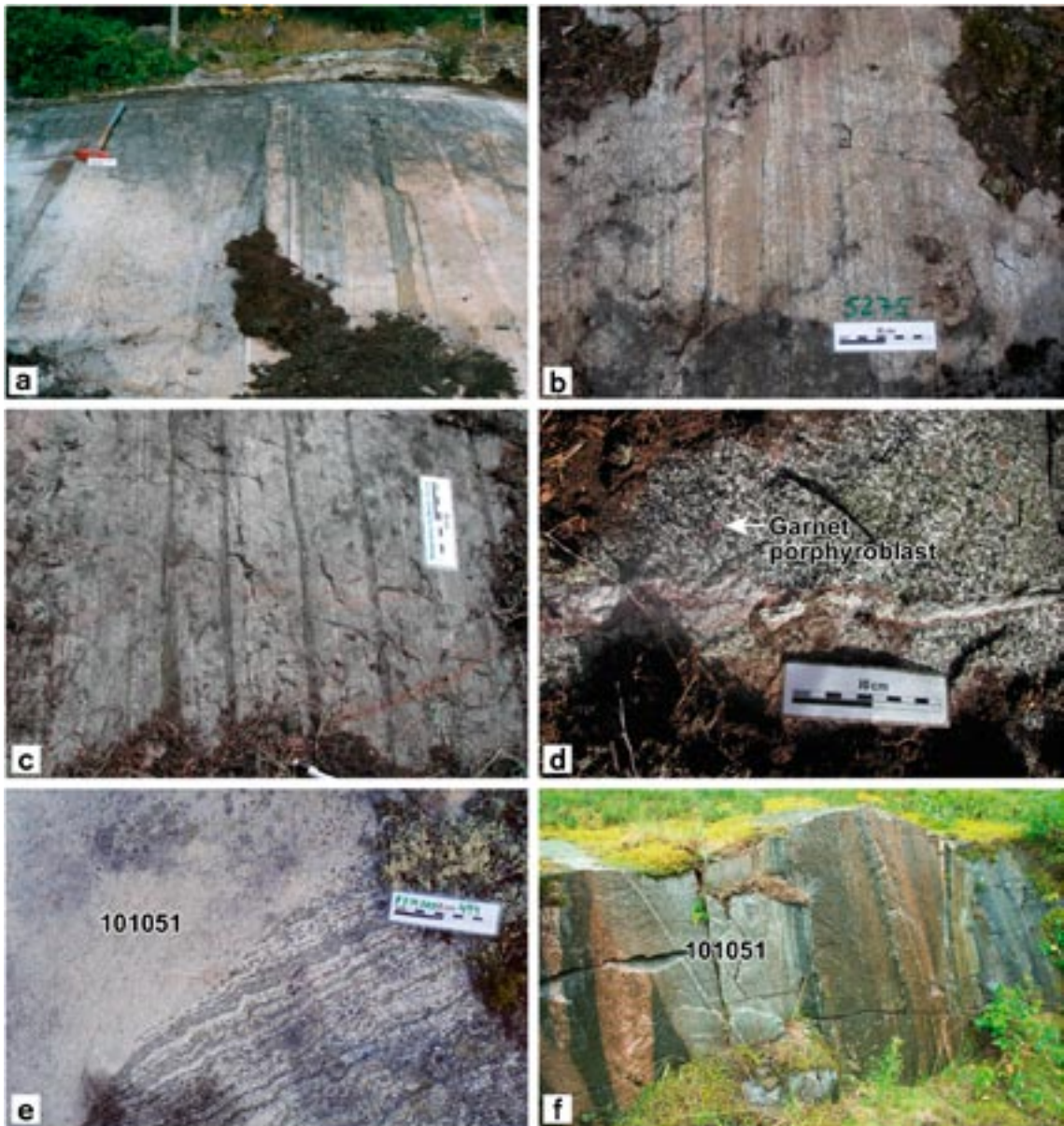


**Figure 5-3.** Field character of the rocks inside subarea 2 in the south-western part of the area selected for mapping at Forsmark. a) Tectonically banded sequence of foliated and lineated metatonalite, felsic metavolcanic rock and amphibolite in ductile high-strain belt. The thin granitic vein to the right in the photograph is mildly discordant to the tectonic banding (observation point PFM000316 close to drill site 4). b) Similar strongly banded Group B metatonalite and amphibolite in ductile high-strain belt (PFM005275). c) Banded and foliated Group A felsic metavolcanic rock in ductile high-strain belt (PFM000775). d) Garnet porphyroblasts in Group B metadiorite (PFM000851). e) Fine- to medium-grained metagranite (101051, Group C) mildly discordant to the tectonic banding in a xenolith of Group B metatonalite and amphibolite (PFM000494). f) Fine- to medium-grained metagranodiorite (101051, Group C) mildly discordant to a tectonically banded sequence of coarser-grained metagranite, amphibolite and pegmatite (PFM001878).

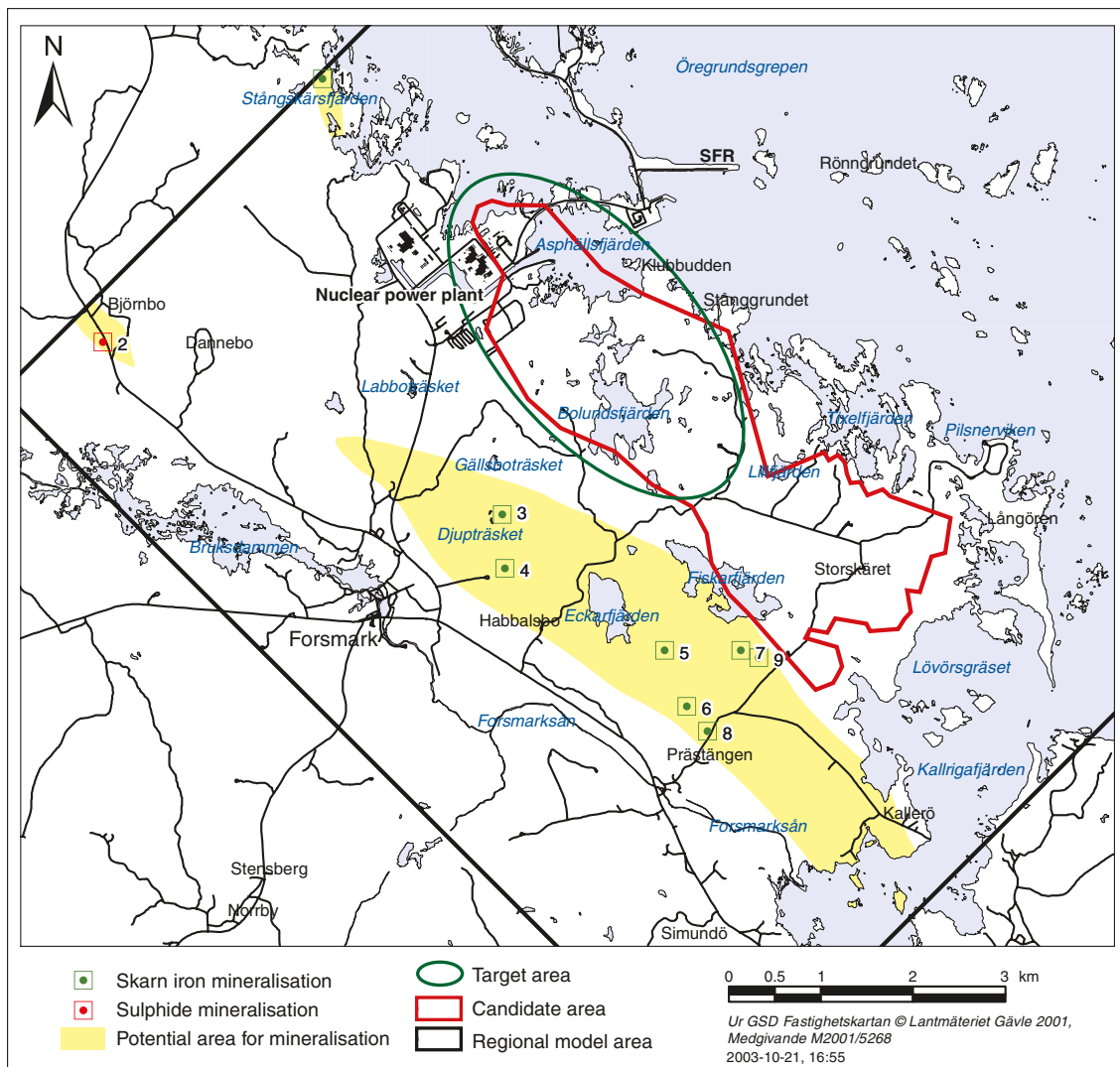


**Figure 5-4.** Mineral resource map of the Forsmark area. The map shows the areas on the surface that are judged to have some exploration potential for mineral deposits (modified after /Lindroos et al. 2004/).

Major bodies of ultramafic rock, metagabbro, metadiorite and quartz-bearing metadiorite (Group B) are also conspicuous in subarea 2 (Figure 4-1). The major gabbroic to dioritic body south-west of the nuclear power plant (Figure 4-1) is locally rich in garnet (Figure 5-3d). As in the south-westernmost part of the mapped area, these quartz-poor rock units have been marked on the geological map with a lens-like geometry.

Two types of younger, minor intrusive rocks comprise subordinate, mappable rock units in the subarea (Figure 4-1). These include grey to reddish grey, fine- to medium-grained metagranodiorite or metatonalite (Group C) and pegmatite, pegmatite granite and fine- to medium-grained granite (Group D). Pegmatite and pegmatitic granite are commonly spatially associated with the lensoid mafic to intermediate bodies. Field relationships on outcrop scale indicate that at least some deformation affected the Group B intrusive rock suite prior to intrusion of the Group C rocks (Figure 5-3e and Figure 5-3f).

### **Ductile structures**

An inhomogeneous bedrock that also displays high ductile strain is conspicuous up to c 1,000 m across the strike, on both sides of the Eckarfjärden and Forsmark deformation zones. In more heterogeneous rock units, the bedrock shows an intense tectonic banding (Figure 5-3a and Figure 5-3b). Both planar and linear structures are present in these areas, i.e. the bedrock is predominantly composed of SL-tectonites. Rotated relics of pegmatite veins in highly-strained rocks in the subarea indicate a component of dextral strike-slip movement (Figure 5-5a). Minor folds, which contain an intense, mineral stretching lineation along the fold axes, deform the ductile planar fabric in these highly-strained rocks (Figure 5-5b). Larger pockets of more homogeneous rocks with an inferred lower degree of ductile deformation are present in the north-western part of the subarea and in the inferred strain shadow close to the major ultramafic-mafic intrusion, in the south-eastern part of the subarea (Figure 5-6). It is inferred that these pockets form tectonic lenses affected by lower ductile strain in a predominantly more highly strained bedrock. The Group B ultramafic, mafic and intermediate plutons, and the Group C minor intrusive rocks are also less distinctly affected by ductile strain. Linear grain-shape fabrics dominate in these rocks.

A concentration of high ductile strain is evident along the Eckarfjärden deformation zone /Stephens et al. 2007/. An intense banding structure (Figure 5-5c), which formed under amphibolite facies metamorphic conditions, is conspicuous in the vicinity of the zone. Even the Group D rocks are affected by intense ductile deformation in the vicinity of the zone (Figure 5-5c). Mylonites as well as extensive hematization and epidotization of the rocks characterise later deformation along the zone under greenschist facies metamorphic conditions (Figure 5-5d). Similar structural features are inferred to be present close to and along the poorly exposed Forsmark deformation zone and drilling along borehole KFM12A have confirmed the complex character of this deformation zone /Carlsten et al. 2007, Stephens et al. 2008/.

In subarea 2, the ductile structures show a regular orientation pattern similar to that observed in the south-westernmost subarea (compare Figure 5-2 and Figure 5-6). There is a dominance of steep planar structures that dip to the south-west and lineations, both mineral stretching lineation and fold axes, plunge moderately to the south-east. Both the amphibolites (Group B) and the younger granitic and pegmatitic dykes (Group D) in the subarea are oriented more or less parallel to the tectonic foliation or banding in the bedrock (Figure 5-6). This is contrast to the situation in the adjacent subareas 1 and 3 where the Group D rocks show a more variable orientation. This feature is inferred to reflect the variation in the degree of ductile strain in the different subareas. Furthermore, it is inferred that ductile strain has continued to affect the bedrock during and after intrusion of the Group D rocks in subarea 2.

### **Geophysical signature**

The south-western part of the mapped area in subarea 2 is characterised by a strongly banded, magnetic anomaly pattern of mostly high intensity (Figure 2-4 and /Isaksson et al. 2004a/) and the magnetic connections trend consistently WNW-ESE to NW-SE. The Forsmark deformation zone corresponds to an elongate, narrow magnetic low that also trends WNW-ESE. For this reason, there are some difficulties in subarea 2 to interpret the geological significance of elongate, narrow, low magnetic units that show this trend. They constitute either a banded, low magnetic bedrock unit or a brittle to brittle-ductile deformation zone. They have been identified as lineaments and assigned a magnetic “minima connection” character in the geophysical interpretation work /Isaksson et al. 2004a/. The problem is illustrated by an elongate, low magnetic unit of minima connection character, located immediately north-east of and parallel to the Forsmark deformation zone (Figure 2-4). In the field, this anomaly has been verified to be caused by metatonalite and amphibolite with low magnetic susceptibilities. There is no evidence for the presence of a brittle or brittle-ductile deformation zone.

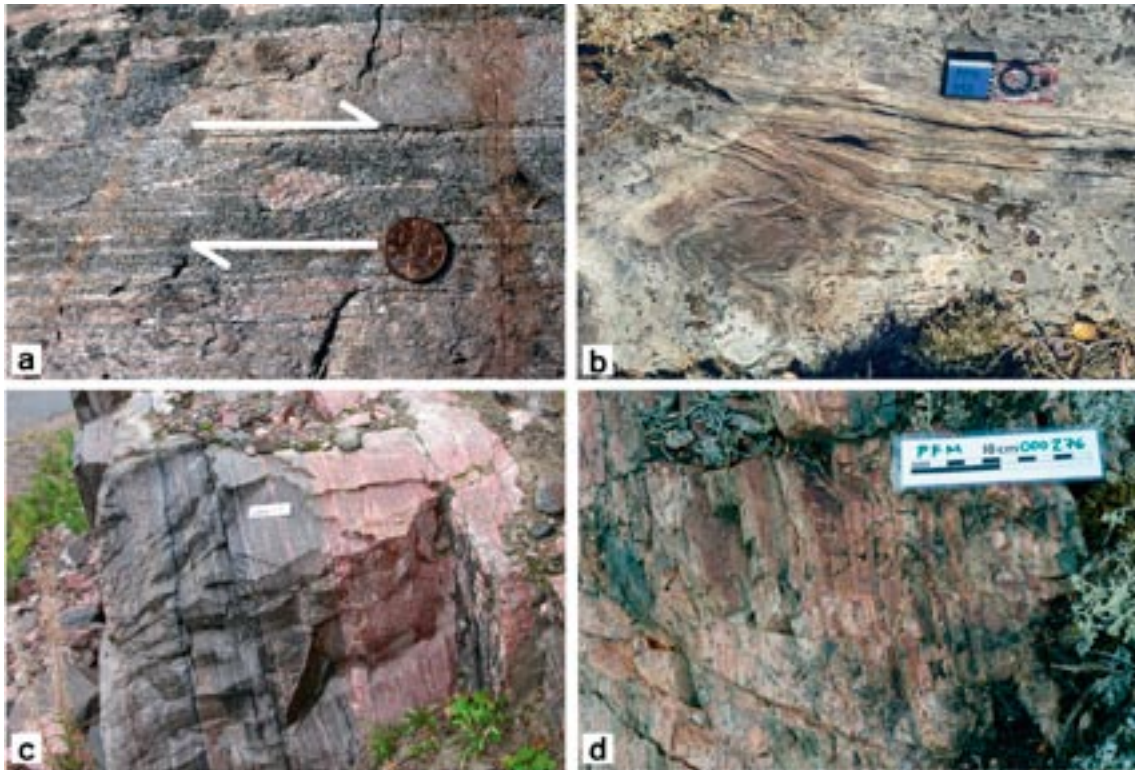


**Figure 5-5.** Ductile structures inside subarea 2 in the south-western part of the area selected for mapping at Forsmark. a) Rotated remnant of a pegmatite vein ( $\delta$ -type) indicating a dextral strike-slip component of movement in the ductile high-strain belt to the south-west of the candidate area (observation point PFM002064). b) Banded and folded Group A felsic metavolcanic rock. Garnet is present in the darker, biotite-rich bands (not visible in photograph). The folds show S-type asymmetry (PFM000392). c) Intense ductile strain under amphibolite-facies metamorphic conditions in the vicinity of the Eckarfjärden deformation zone (PFM000834). The pinkish rock to the right in the photograph is pegmatitic granite. This rock is also affected by the intense ductile strain. d) Low-temperature mylonite and strong hematisation/epidotisation along the Eckarfjärden deformation zone (PFM000276).

In the south-eastern part of the subarea, an ultramafic intrusion correlates with a strong, circular magnetic anomaly with an irregular pattern (Figure 2-4). Some of the high magnetic connections in subarea 2 are related to magnetite mineralisation.

Large parts of subarea 2 show a moderate to high intensity on the airborne gamma-ray spectrometry map, related to an increase in potassium, uranium and/or thorium contents at the ground surface (Figure 2-6 and /Isaksson et al. 2004a/). Smaller areas with high intensity correspond well with exposed pegmatitic rocks /Isaksson et al. 2004a/. Larger areas where ultramafic, mafic and intermediate rocks are exposed show low gamma-ray intensity.

The Bouguer anomaly map (Figure 2-7) indicates that subarea 2 is located on a steep, NW-SE oriented gradient in the gravity field. This means that the subarea constitutes a transition zone between a moderate to high gravity plateau to the south-west (see section 5.2.1) and a gravity low to the north-east caused by larger volumes of low density rocks (see section 5.2.3). A local gravity minimum, south of the Forsmark nuclear power plant, indicates a local mass deficiency and possibly corresponds to an occurrence of Group C rocks of granitic to granodioritic composition and subordinate Group D pegmatitic rock. However, the outcrop frequency in this area is poor and the correlation is uncertain.



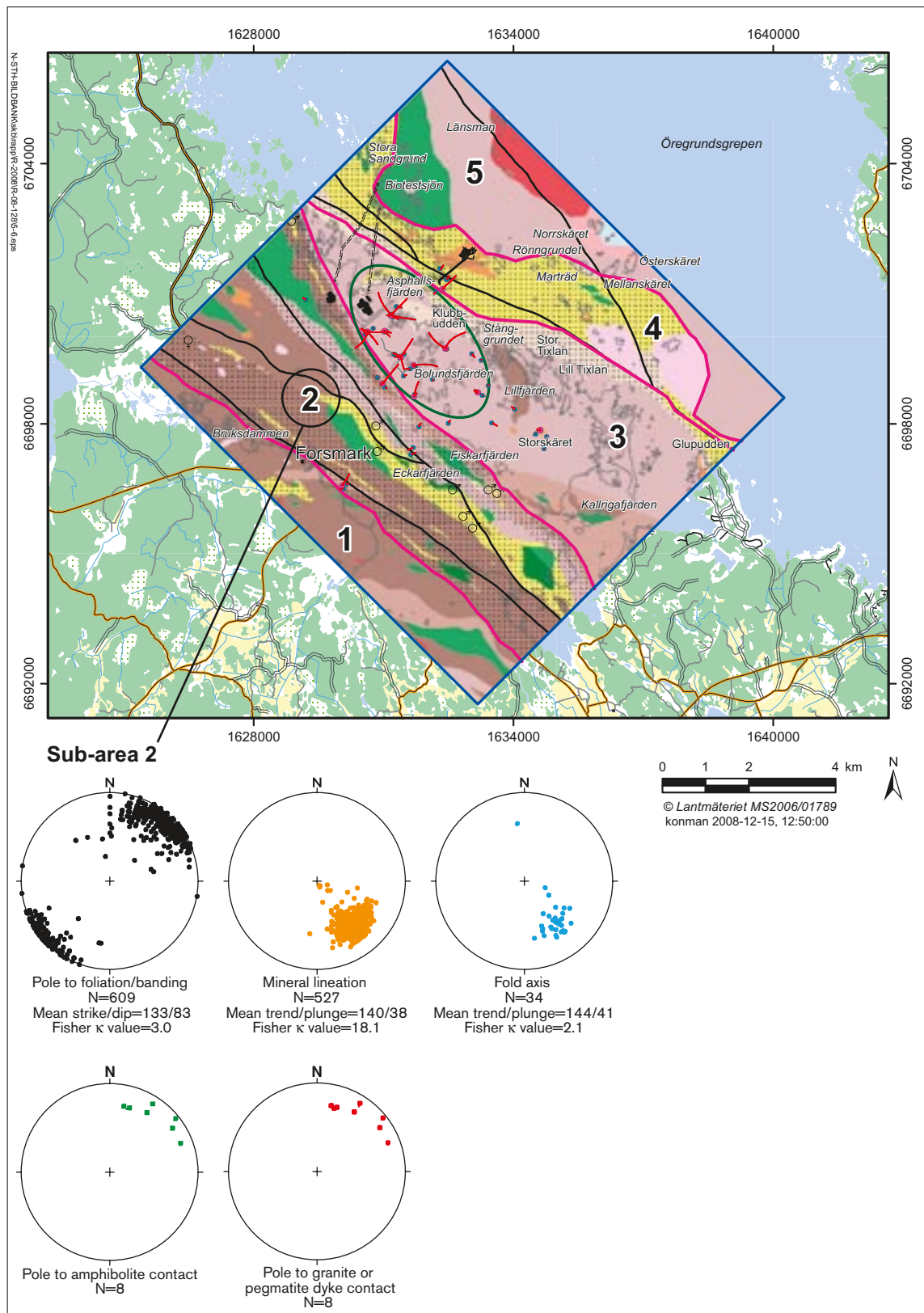


**Figure 5-6.** Orientation of ductile structures, amphibolites and Group D granitic and pegmatitic dykes at the ground surface in subarea 2. All structures and rock contacts have been plotted on the lower hemisphere of a Schmidt, equal-area stereographic projection. Planar structures and rock contacts have been plotted as poles to planes. The stereographic projections for the ductile structures are taken from /Stephens et al. 2003b/. The base map is the bedrock geological map of the area (see Figure 4-1 for legend).

Immediately north-west of the mapped area, a locally strong gravity high indicates a large mass excess in a limited area. Rocks with gabbroic to dioritic composition are present in this area, but due to the local character of the gravity anomaly and its intensity, the occurrence of a mineralisation cannot be excluded (see also /Isaksson and Stephens 2007/). The gravity maximum also corresponds to a magnetic low. The cause of this anomaly lies outside the mapped area and has not been assessed in more detail in the field.

### 5.2.3 Subarea 3 in the central part of the mapped area including the candidate and target areas

#### *Lithology*

Subarea 3 in the central part of the mapped area, which includes the candidate and target areas (Figure 4-1), is dominated by medium-grained metagranite (Figure 5-7) that belongs to the Group B suite of intrusive rocks (Table 4-1, Figure 4-1 and Figure 4-2). Although amphibolite, fine- to medium-grained metagranitoid (Group C) and pegmatitic granite, pegmatite and fine- to medium-grained granite (Group D) commonly form subordinate components at outcrop scale (Figure 5-7), this rock unit is relatively homogeneous. A conspicuous variation at the surface is an increase in the proportion of pegmatitic granite and pegmatite to the south-east, in the area around Storskäret.

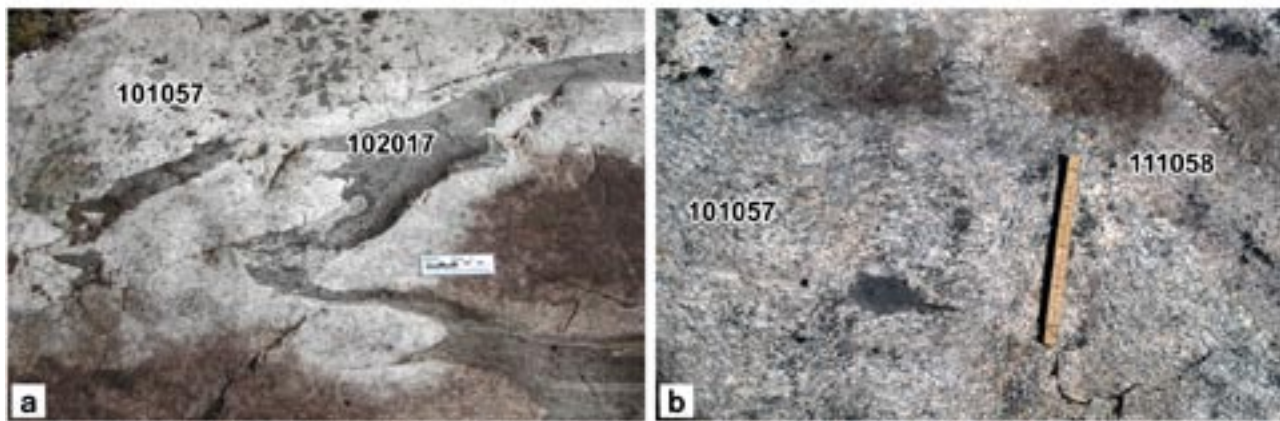


*Figure 5-7. Dominant medium-grained metagranite and subordinate rock types that together form the most prominent rock unit inside subarea 3 in the central part of the mapped area. This rock unit strongly dominates the candidate and target areas at Forsmark. a) Folded tectonic foliation and rock contact between Group B metagranite (101057) and amphibolite (102017) south-west of drill site 5, in the south-western, marginal part of subarea 3 (observation point PFM0001164). b) Folded tectonic foliation with minor shear zone development in Group B metagranite (101057) close to drill site 6 (observation point PFM001176). The tectonic foliation is strongly discordant to a Group D granite dyke (111058).*

Subarea 3 also contains several other, more subordinate mappable rock units:

- A large-scale xenolith of Group B metatonalite (Figure 5-8a) is situated close to Lillfjärden, predominantly outside the candidate area and outside the target area (Figure 4-1). This rock unit is deformed in an open fold structure (Figure 4-1).
- A heterogeneous mixture of metagranodiorite and metatonalite with subordinate meta-gabbro, metadiorite, pegmatitic granite and pegmatite is situated in the south-eastern part of subarea 3. This rock unit also occurs predominantly outside the candidate area and outside the target area (Figure 4-1).
- Group B aplitic metagranite is situated close to and along the southern shore of Asphällsfjärden, inside both the candidate and target areas, and is inferred to lie in the hinge of a major fold structure (Figure 4-1 and Figure 4-2).
- West and north of Asphällsfjärden, including the area beneath reactor site 1 and 2, the bed-rock is defined by an heterogeneous mixture of Group A felsic metavolcanic rock, Group B aplitic metagranite, medium-grained metagranite and amphibolite, Group C metagranodiorite and Group D pegmatitic granite, pegmatite and granite (Figure 4-1 and Figure 4-2). This heterogeneous rock unit, which is affected by a high degree of ductile strain (Figure 5-8b), is inferred to continue to the south-east and is well-exposed along the coast (Figure 4-1) at Klubbudden (Figure 5-8c), Stånggrundet, Stor Tixlan, Lill Tixlan and Glupudden (Figure 5-8d). The outline of this complex rock unit at the ground surface, which is situated outside both the candidate and target areas, defines a major fold structure inside subarea 3 (Figure 4-1 and Figure 4-2).

The Group B aplitic metagranite around Asphällsfjärden and within the heterogeneous rock unit west and north of Asphällsfjärden and along the coast between Klubbudden and Glupudden shows a distinctive sugary texture, a leucocratic appearance with only occasional thin seams of biotite and the absence of a distinctive tectonic foliation. However, the rock shows a diffuse banding defined, in part, by subtle changes in rock colour between more reddish and paler, more whitish varieties (Figure 5-8d). As indicated above, the aplitic metagranite is tectonically interleaved with a variety of other rock units in the heterogeneous rock unit along the coast (Figure 4-2), including Group B medium-grained metagranite similar to that observed inside the candidate area in the central part of subarea 3. Whitish rock with isolated aggregates of biotite is present in this rock unit as well as in the medium-grained metagranite beneath reactor site 1 and 2 (Figure 5-8e). The same type of bleached rock with isolated aggregates of biotite also occurs as contact rims adjacent to amphibolite (Figure 5-8f).

It has been inferred that the bleaching in both types of granite was related to hydrothermal alteration at an early stage in the geological evolution /Stephens et al. 2003b, 2005/. The alteration is absent in the younger Group C rocks. This interpretation has been confirmed by drill core data where the early hydrothermal alteration is referred to as albitization /Pettersson et al. 2005/. The alteration resulted in a change in colour to paler more whitish varieties, an elimination of rock contrast based on grain-size, a loss of  $K_2O$  and a resultant tendency towards a pseudo-granodioritic or pseudo-tonalitic composition. For this reason, some difficulties arise concerning which type of granite has been affected by the alteration. It has been suggested that this type of alteration is a pervasive feature in parts of the older felsic rocks. Furthermore, it is a pre- or possibly syn-metamorphic feature that was triggered by the heat supply provided by the intrusion of younger igneous rocks including amphibolite in Group B and metagranitoids in Group C /Pettersson et al. 2005, Stephens et al. 2007/.

On Klubbudden, the Group C minor intrusions are mildly discordant to the intense tectonic banding in the host rocks (Figure 5-9a). By contrast, the granite dykes and some of the pegmatites that are included in the Group D rocks are strongly discordant to this tectonic banding (Figure 5-9b). Such field relationships between the younger Group C and Group D intrusive rocks and the penetrative ductile strain have also been observed at other outcrops inside subarea 3 (see, for example, Figure 5-7b).

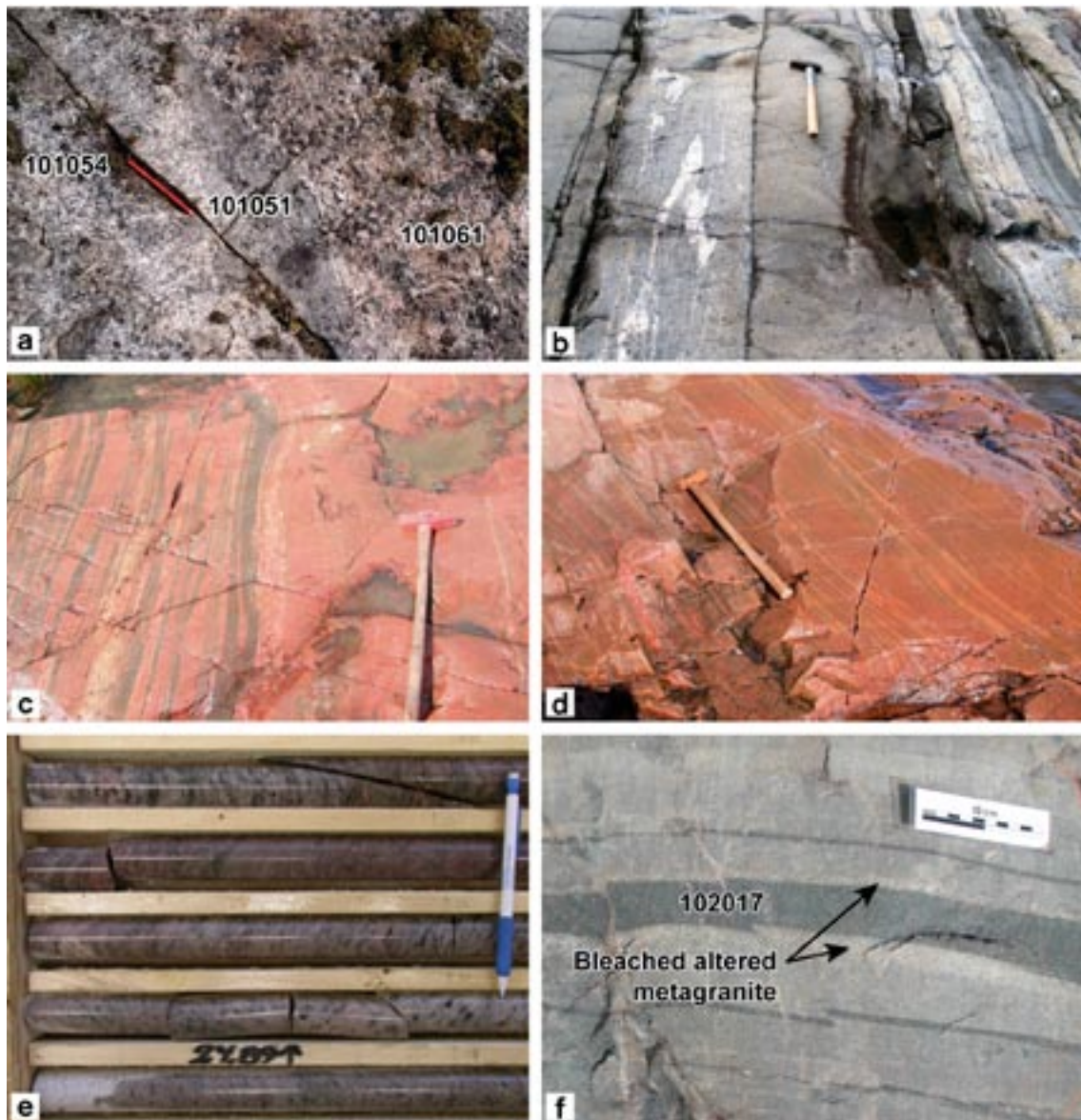


**Figure 5-8.** Field character of the rocks in subordinate rock units inside subarea 3 in the central part of the mapped area. a) Lineated and weakly foliated medium-grained Group B metatonalite (101054), intruded by Group C finer-grained metatonalite (101051), which, in turn, is intruded by Group D pegmatite (101061). This rock unit forms a folded large-scale xenolith inside the dominant Group B metagranite unit in subarea 3 (observation point PFM001162). b) Tectonically banded, foliated and lineated meta-igneous rocks with intra-folial folds in the folded ductile high-strain belt north of Asphällsfjärden (PFM001220). c) Tectonically banded aplitic metagranite, amphibolite and pegmatite in the folded ductile high-strain belt on Klubbudden (PFM000732). Note the subordinate, paler, whitish bands in the generally reddish, Group B aplitic metagranite. d) Tectonically banded, Group B aplitic metagranite in the same ductile high-strain belt as that exposed on Klubbudden (PFM001689). Note the distinctive banding with reddish and paler, whitish varieties of the aplitic metagranite. e) Biotite aggregates in altered and whitish, medium-grained Group B metagranite (shallow borehole KFK116 beneath reactor site 1 and 2. Corresponds to borehole D4 using older nomenclature). f) Bleached, altered Group B metagranite along the contact to an amphibolite dyke (PFM000776).

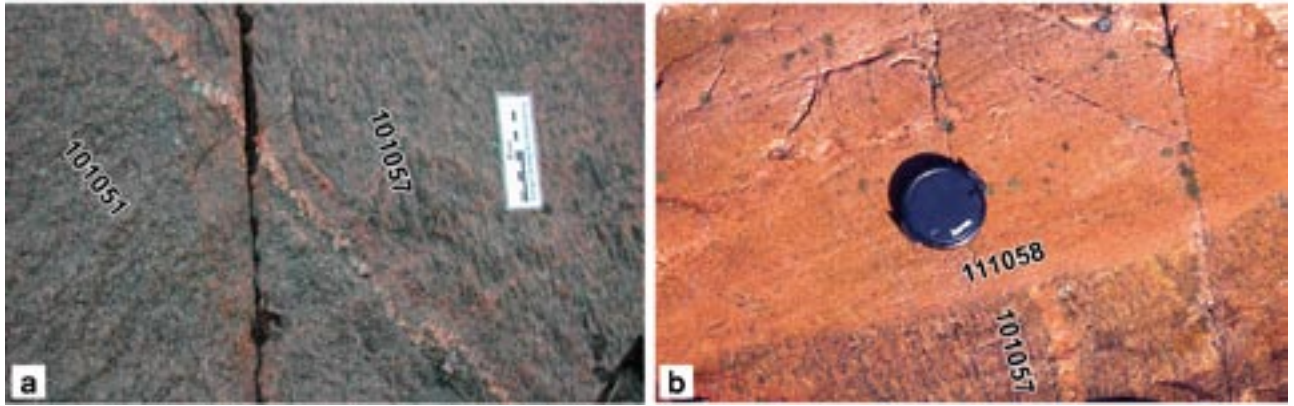


**Figure 5-9.** Field relationships between the intrusion of the younger Group C and Group D rock groups and the ductile deformation and metamorphism in their Group B host rocks. a) Boudin of Group C fine- to medium-grained metagranodiorite (101051) with a linear grain-shape fabric, mildly discordant to the intensely tectonic banded Group B host rock including metagranite (101057) and amphibolite (observation point PFM000718). b) Dyke of Group D granite (111058) strongly discordant to penetratively and strongly foliated Group B metagranite (101057) (observation point PFM001033).

### **Ductile structures**

The bedrock in the central part of the mapped area in subarea 3 is generally affected by a lower level of ductile deformation relative to that observed in the adjacent areas to the south-west and north-east, i.e. subareas 2 and 4, respectively. A linear grain-shape fabric with subordinate, planar structures dominates in the subarea, i.e. the bedrock is predominantly composed of LS-tectonites. The folded high-strain unit with a heterogeneous rock composition that extends from west and north of Asphällsfjärden and along the coast between Klubbudden and Glupudden is an exception. Overall the bedrock belongs to a major tectonic lens (Forsmark tectonic lens) sandwiched between the generally more highly strained rocks in subareas 2 and 4 with WNW-ESE to NW-SE strike direction.

As indicated above, the distribution of rock units on the bedrock geological map (Figure 5-10) provides evidence for major folding inside subarea 3. On a smaller scale, outcrop observations indicate that the amphibolites that intrude the metagranite are folded (Figure 5-7a). Furthermore, folding of the penetrative tectonic foliation with an inferred fold axis that plunges moderately to the south-east (134/44) is also indicated from the outcrop data (Figure 5-10). Both the mineral stretching lineation and the measured fold axes also plunge moderately to the south-east (Figure 5-10) and it is apparent that fold axes are sub-parallel to the mineral stretching direction in the bedrock. The smaller-scale features indicate that the major folding is synformal in character in the north-western part of subarea 3, where the target area is situated, and antiformal in character further to the south-east, i.e. the fold is tube-like in character. These geometric features are reminiscent of oblique folds /Passchier and Trouw 1998/ or tubular-shaped structures that are referred to as sheath folds /Cobbold and Quinquis 1980/.

Amphibolites appear to follow the orientation of the planar ductile structures whereas, in sharp contrast to subarea 2, the younger granitic and pegmatitic dykes (Group D) show a more variable orientation (Figure 5-10).

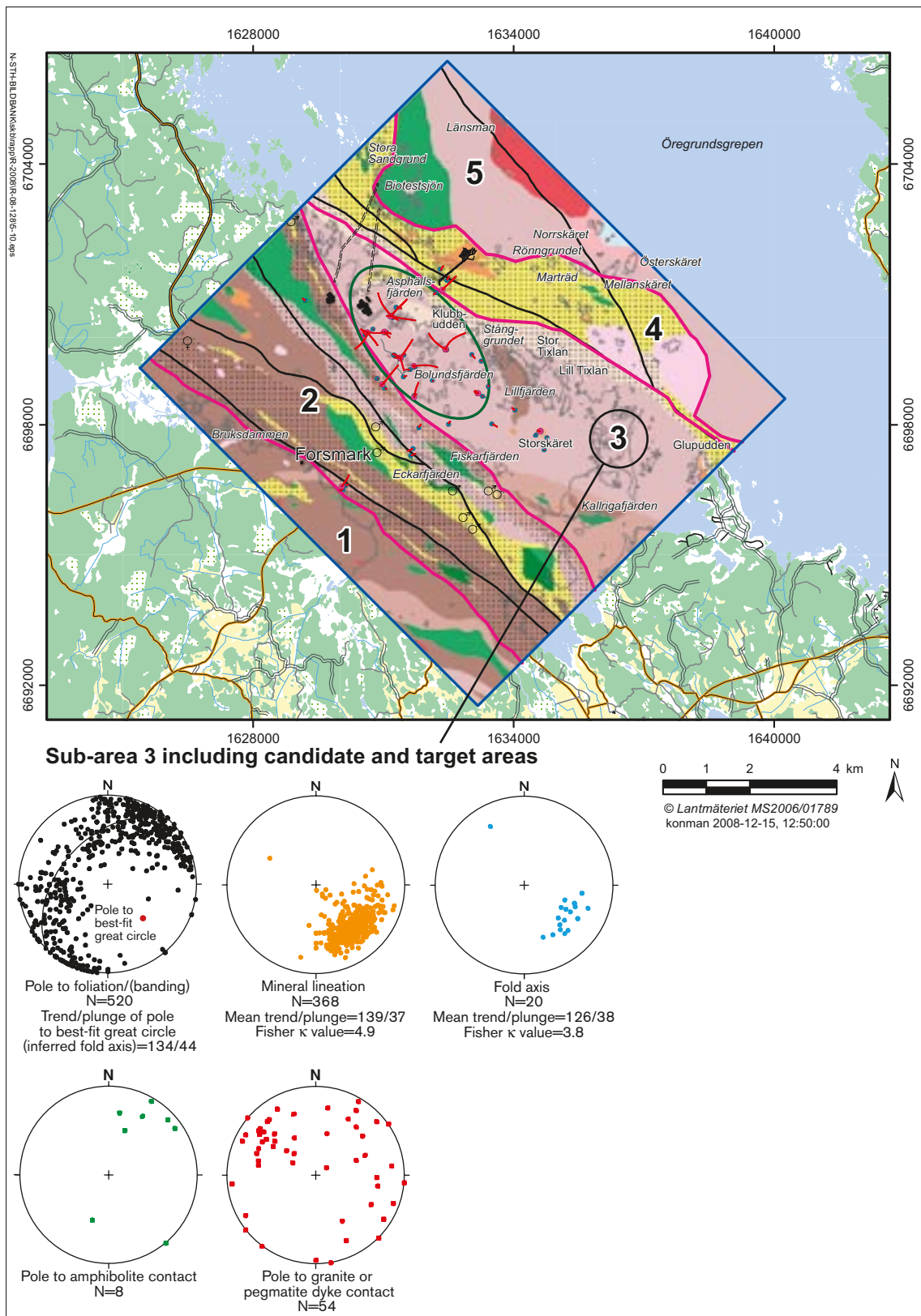


**Figure 5-10.** Orientation of ductile structures, amphibolites and Group D granitic and pegmatitic dykes at the ground surface in subarea 3. All structures and rock contacts have been plotted on the lower hemisphere of a Schmidt, equal-area stereographic projection. Planar structures and rock contacts have been plotted as poles to planes. The stereographic projections for the ductile structures are taken from /Stephens et al. 2003b/. The base map is the bedrock geological map of the area (see Figure 4-1 for legend).

### **Geophysical signature**

The central part of the mapped area in subarea 3 is characterised by an irregular or weakly banded, magnetic anomaly pattern of moderate to low intensity (Figure 2-4 and /Isaksson et al. 2004a/). The north-western part shows a somewhat higher magnetic intensity than the remainder of the subarea. However, petrophysical investigations have shown that this variation can be accommodated for by the range in values for magnetic susceptibility in the medium-grained metagranite that constitutes the main rock type in this subarea /Isaksson et al. 2004b/. Magnetic connections constructed on the basis of the high-resolution ground magnetic data (Figure 2-5 and /Isaksson et al. 2007/) confirm the major folding inside subarea 3.

Areas characterised by low magnetic anomalies correlate mainly with subordinate rock units, i.e. the rock unit dominated by Group B metatonalite close to Lillfjärden, the folded metavolcanic and pegmatitic rocks inside the heterogeneous rock unit to the west and north of Asphällsfjärden, and the occurrence of Group B aplitic metagranite close to and along the southern shore of Asphällsfjärden. An elongate SW-NE oriented magnetic low beneath the sea in Kallrigafjärden in the south-eastern part of the subarea is also present. The geological feature that gives rise to this anomaly is not known.

Apart from the candidate area, a major part of subarea 3 is covered by seawater and, hence, no information is available from the gamma-ray spectrometry data (Figure 2-6 and /Isaksson et al. 2004a/). The distribution of different inferred thorium-potassium-uranium levels within the Forsmark candidate area is characterised by three distinct patterns:

- From Bolundsfjärden to Fiskarfjärden and around drill site 2, background and/or low thorium-potassium-uranium intensity levels are conspicuous.
- Around Storskäret, in the south-eastern part of the candidate area, thorium and potassium dominate and commonly show rather high intensities. This class corresponds to the well-exposed farmland at Storskäret where clay-rich till has been observed /Sohlenius et al. 2004/. However, it also corresponds to a more upland terrain which is partly rich in boulders and contains fairly large outcrop areas.
- The target area between Bolundsfjärden and the nuclear power plant and further to the north-west shows a clear thorium and uranium dominance. The intensities of these components are also relatively high around drill site 1 and to the south-west of this drill site. The low potassium content in this area is consistent with the occurrence of the regional hydrothermal alteration discussed above that resulted in depletion of potassium in the bedrock.

Subarea 3 is characterised by a gravity low on the Bouguer anomaly map (Figure 2-7). This gravity low corresponds to the occurrence of the most significant rock unit in the subarea that is dominated by metagranite. As expected, the rock unit dominated by metatonalite close to Lillfjärden, in the central part of the subarea, constitutes a minor gravity high (Figure 2-7).

#### **5.2.4 Subarea 4 in the north-eastern part of the mapped area**

##### ***Lithology***

A rock unit dominated by fine-grained and commonly banded, Group A supracrustal rocks rich in quartz and feldspar (Figure 5-11a), which are interpreted to be volcanic in origin, forms the most prominent rock unit in the north-eastern part of the mapped area in subarea 4 (Figure 4-1). These rocks are predominantly dacitic in composition; some bands show a darker colour and have been judged to be more andesitic. On account of the high degree of deformation and metamorphism, it is uncertain whether these banded rocks should be classified as resedimented, syn-eruptive volcanoclastic or volcanogenic sedimentary deposits. They have been included here in the volcanic rock unit.

Although these rocks are relatively homogeneous in appearance, partly coarser, paler and more homogeneous varieties that contain an increased content of muscovite, occasionally in the form of cm-large porphyroblasts, are present in the northern part of the subarea. Locally, on a small island north-east of Stora Sandgrund, small aggregates up to 0.5 m in diameter are present. These are composed of plagioclase feldspar, quartz and muscovite with subordinate magnetite and garnet (Figure 5-11b). Complementary thin-section work has also revealed the occurrence of fibrolite (sillimanite) in such aggregates /Stephens et al. 2005/. These features have been interpreted to be related to synvolcanic hydrothermal alteration prior to amphibolite-facies metamorphism. Such alteration is a common feature of the metavolcanic rocks in the Bergslagen region, in the central part of Sweden /e.g. Lundström 1995/. Minor bodies of mafic to intermediate rocks with a gabbroic or dioritic composition, commonly amphibolitic, are also present inside the felsic metavolcanic rock unit (Figure 4-1).

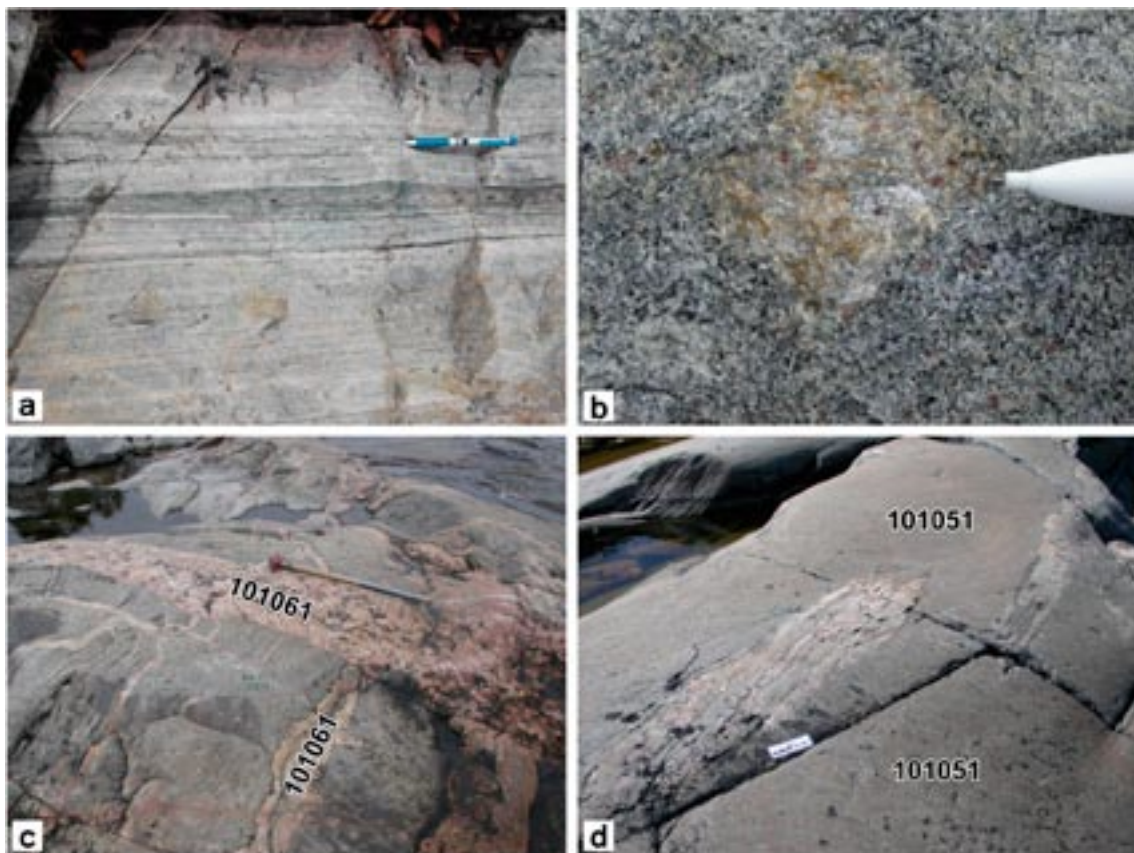


**Figure 5-11.** Field character of the rocks inside subarea 4 in the north-eastern part of the area selected for mapping at Forsmark. a) Banded, foliated and lineated Group A felsic metavolcanic rock in ductile high-strain belt (observation point PFM001110). Compare Figure 5-3c. b) Mineral aggregate composed of plagioclase feldspar, quartz and muscovite with subordinate magnetite and garnet in Group A felsic metavolcanic rock (observation point PFM005212). The aggregate is inferred to represent a metamorphosed alteration rock. c) Foliated and lineated Group A felsic metavolcanic rock in ductile high-strain belt with both concordant and strongly discordant veins or dykes of pegmatite (101061). The occurrence of different generations of pegmatite is apparent (observation point PFM005241). d) Xenoliths of migmatitic meta-igneous rocks with pegmatitic neosome inside a weakly deformed Group C metagranodiorite (101051) (observation point PFM005234).



Group D pegmatite in the form of concordant veins along the tectonic foliation and younger, discordant dyke-like bodies (Figure 5-11c) or more homogeneous mappable rock units (Figure 4-1) comprise a highly significant rock component in the felsic metavolcanic rocks in the north-eastern part of the mapped area. One such unit has been identified in the vicinity of the SFR facility (Figure 4-1). Field relationships indicate that the pegmatites intruded the supracrustal rocks and were not formed by *in situ* partial melting of their direct host rock. One exception occurs in the dacitic metavolcanic rocks on Rönnggrund, in the central part of the subarea, where pegmatite veins and leucogranite have been interpreted as a neosome in a migmatitic variety of the felsic metavolcanic rocks.

Several islands in the south-eastern part of subarea 4 are completely dominated by fine- to medium-grained, equigranular metagranodiorite included in the Group C meta-igneous suite. Two separate bodies have been inferred to be present and are included on the geological map (Figure 4-1). However, the lateral extension of these rock units at the ground surface is poorly constrained due to the restricted number of outcrops and the lack of distinctive anomalies provided by the airborne geophysical data. The Group C meta-igneous rocks only show a linear grain-shape fabric and contain inclusions of migmatitic felsic metavolcanic rock (Figure 5-11d). The volcanic component in the palaeosome in these inclusions is inferred to have a dacitic composition and the neosome is composed of pegmatitic veins (Figure 5-11d).

### **Ductile structures**

The bedrock in the north-eastern part of the mapped area in subarea 4 shows a high level of ductile strain and contains both planar and linear ductile structures. The consistently linear grain-shape fabric in the Group C meta-intrusive rocks forms an important exception to this general rule. Subarea 4 is also the host to the regionally important Singö deformation zone with its splays to the north.

Winged porphyroclasts /Passchier and Trouw 1998/ in highly-strained rocks affected by amphibolite-facies metamorphism indicate a component of dextral strike-slip ductile shear deformation (Figure 5-12a). This kinematics is similar to that observed in subarea 2 on the south-western flank of the major fold structure inside subarea 3. Minor folds, which contain an intense, mineral stretching lineation along the fold axes, deform the planar fabric in these highly-strained rocks (Figure 5-12b). Eye-shaped, tubular folds have also been observed at some localities in subarea 4 (Figure 5-12c). Ductile shear bands in protomylonitic pegmatite inside the high-strain belt that hosts the Singö deformation zone show a dextral strike-slip component of displacement (Figure 5-12d). This locality is also situated along a zone that splays away from the Singö deformation zone on its northern side. Although these shear bands formed at a lower grade of metamorphism compared with the highly strained rocks in the subarea that formed under amphibolite-facies metamorphic conditions, they show the same kinematics.

The poles to the planar grain-shape fabric in the north-eastern part of the mapped area are aligned along a great circle in a stereographic projection plot (Figure 5-13). This feature is suggested to be steered by the folding of these structures around the major body of metadiorite in subarea 5 in the northernmost part of the mapped area (Figure 5-13). The pole to this great circle, which is inferred to represent the fold axis, plunges steeply to the south-east (129/62). Both the mineral stretching lineation and the measured fold axes in subarea 4 show a variable orientation with a gentle to steep plunge to the south-east (Figure 5-13). Orientation data for the Group D granite and pegmatite dykes indicate that these rocks also show a variable orientation (Figure 5-13). However, the dip direction is predominantly to the south and east, i.e. the poles to rock contacts plot mainly in the north-western quadrant on the stereographic projection plot (Figure 5-13).

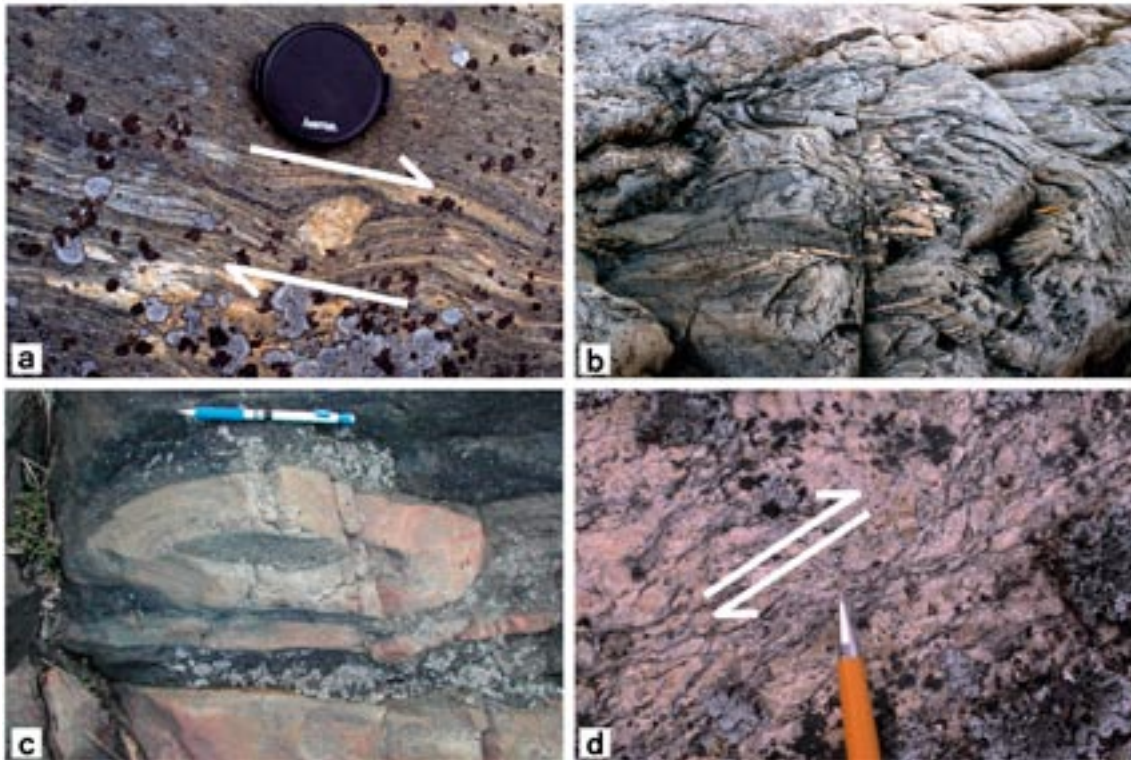


**Figure 5-12.** Ductile deformational structures inside subarea 4 in the north-eastern part of the area selected for mapping at Forsmark. a) Winged porphyroclast ( $\delta$ -type) indicating a dextral strike-slip component of movement in ductile high-strain belt (observation point PFM001235). b) Folded Group A felsic metavolcanic rock in ductile high-strain belt. The folds show gently dipping fold axes (close to observation point PFM001900). c) Eye-shaped tubular fold along ductile high-strain belt (PFM001684). d) Shear bands (close to the pen tip) in Group D pegmatitic granite affected by low-temperature ductile deformation along the ductile high-strain belt that hosts the Singö deformation zone and its splays to the north. The relationship between the shear bands and the main shear surfaces indicates a dextral strike-slip component of movement (PFM001637).

### **Geophysical signature**

The north-eastern part of the mapped area in subarea 4 is characterised by a banded magnetic anomaly pattern of mostly moderate intensity (Figure 2-4 and /Isaksson et al. 2004a/). The magnetic connections generally trend WNW-ESE and the Singö deformation zone occurs as an elongate, well-defined magnetic low (Figure 2-4). In the north-western part of the subarea, the magnetic bands change orientation and trend in a south-north direction. In this area, a magnetic band of high intensity correlates with felsic to intermediate metavolcanic rocks with high magnetic susceptibility. Similar magnetic highs are also present close to subarea 5 in the central part of the subarea. These anomalies are covered by seawater and it has not been possible to evaluate their origin with the help of field data. Since most of the subarea is covered by seawater, no information is available from the gamma-ray spectrometry data (Figure 2-6 and /Isaksson et al. 2004a/).

The Bouguer anomaly map shows that the gravity low observed in the central part of the mapped area in subarea 3 continues to the north-east beneath the sea (Figure 2-7). However, since felsic to intermediate metavolcanic rocks are inferred to be the dominant rock type in this area, the mass deficiency indicates that either these rocks are strongly felsic in composition or the occurrence of felsic intrusive rocks, including pegmatite and/or pegmatitic granite, is underestimated at the surface or in the continuation of subarea 4 at shallow depth. A distinct gravity low in the area around the SFR repository corresponds to a significant occurrence of pegmatite and/or pegmatite granite (Figure 4-1). The magnetic highs that occur close to subarea 5 in the central part of the subarea correspond to a local gravity high, which indicates the occurrence of a rock type with higher density.

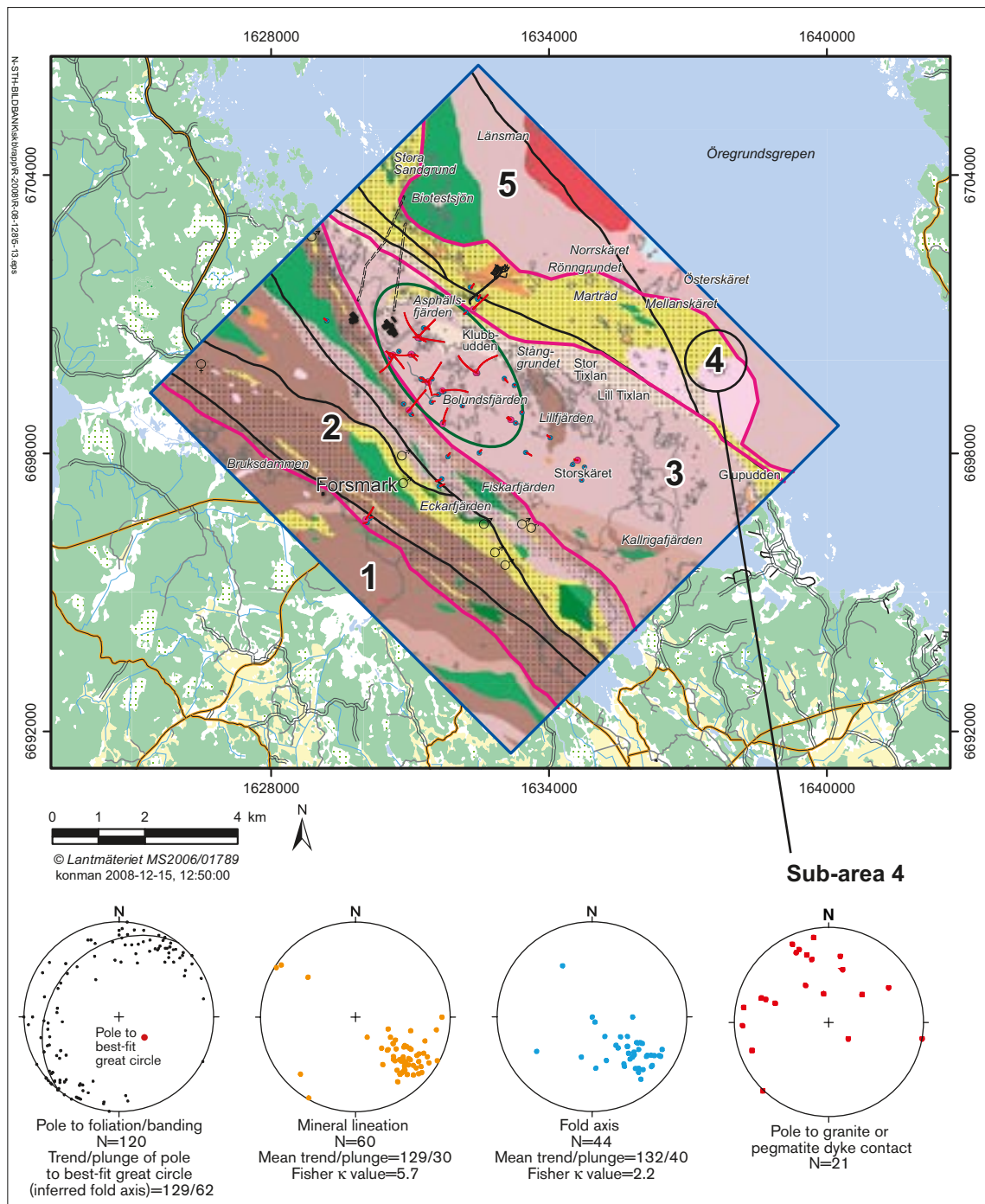


**Figure 5-13.** Orientation of ductile structures and Group D granitic and pegmatitic dykes at the ground surface in subarea 4. All structures and rock contacts have been plotted on the lower hemisphere of a Schmidt, equal-area stereographic projection. Planar structures and rock contacts have been plotted as poles to planes. The stereographic projections for the ductile structures are taken from /Stephens et al. 2003b/. The base map is the bedrock geological map of the area (see Figure 4-1 for legend).

## 5.2.5 Subarea 5 in the north-easternmost part of the mapped area

### *Lithology*

The north-easternmost part of the mapped area in subarea 5 predominantly lies beneath the sea and the subarea contains relatively few observation points. Metagranite dominates in what is inferred to be the most prominent rock unit and is well-exposed on the islands referred to as Marträäd, Mellanskäret and Österskäret in the central part of subarea 5 (Figure 4-1). This lithology belongs to the Group B intrusive rock suite and is similar to that observed inside subarea 2 and in the candidate area inside subarea 3. The metagranite is generally medium-grained, strongly lineated and foliated (L>S tectonite). The boundary to the west towards fine-grained, banded metagranite on, for example, the island Marträäd (Figure 4-1) is not distinct. Furthermore, the transition into more migmatitic metagranite with veins of leucocratic, fine-grained granite and pegmatite, which form a neosome in the migmatite, can be observed in the central part of the island Österskäret (Figure 4-1). The central and north-eastern part of subarea 5 is generally characterised by migmatitic rocks (Figure 4-1 and Figure 5-14a).

A homogeneous, medium-grained, more or less isotropic to weakly lineated quartz-bearing metadiorite to metagranite dominates a conspicuous rock unit in the north-westernmost part of the subarea, i.e. in the eastern part of the area referred to as Biotestsjön (Figure 4-1). This unit resembles the intermediate, mafic and ultramafic bodies that belong to the Group B igneous suite in subarea 2. Minor ductile shear zones up to a few centimetres thick and with a highly variable strike are common within the metadioritoid (Figure 5-14b). It is intruded by abundant pegmatite dykes and both dykes and minor bodies of fine- to medium-grained metagranodiorite that belongs to the Group C intrusive suite.

A major body of medium- and even-grained, grey-red to red granite is present in the north-eastern part of subarea 5 (Figure 4-1). This rock unit is exposed on the island referred to as Länsman as well as on some smaller islands to the south of Länsman. In general, this granite is isotropic or displays only a weak grain-shape fabric and is devoid of dykes and irregular bodies of amphibolite. However, it contains xenoliths of felsic metavolcanic rocks with an inferred dacitic composition and both the host granite and the xenoliths occur in approximately equal proportions on one of the small islands south of Länsman. Sillimanite porphyroblasts are a common feature in one of the xenoliths. The granite is commonly intruded by pegmatite dykes that are several decimetres to 1 m in width (Figure 5-14c). Close to the contacts with pegmatite, the granite is more strongly foliated and affected by some recrystallisation. In the central part of the island Länsman, the granite is also intruded by a fine-grained granite dyke included in the Group D intrusive suite. There remains some uncertainty concerning to which suite of intrusive rocks the medium- and even-grained granite belongs. Bearing in mind its structural character in combination with the absence of amphibolite, it has also been included in the Group D suite on the geological map (Figure 4-1).

A complex mixture of different rock types is present in the north-easternmost part of the subarea on the island referred to as Norrskäret (Figure 4-1). Migmatitic metagranite, including both the medium-grained and sugary, finer-grained varieties, similar to that observed in subarea 3, and grey, fine-grained, banded and strongly folded, biotite-rich supracrustal rocks (Figure 5-14d), inferred to be sedimentary in origin, are present. Pegmatite in the form of both neosome veins in the migmatitic rocks as well as discordant pegmatite dykes is common. Migmatitic meta-sedimentary rock is also present on the small island south-east of Norrskäret (Figure 4-1) where it is intruded by fine- to medium-grained, weakly deformed metagranitoid that belongs to the Group C intrusive suite. Such Group C rocks dominate the northern part of this island and are also present on the adjacent small islands. As in subarea 4, it is apparent that the Group C rocks intruded after the development of migmatites that are exposed at the crustal level represented by the current ground surface.

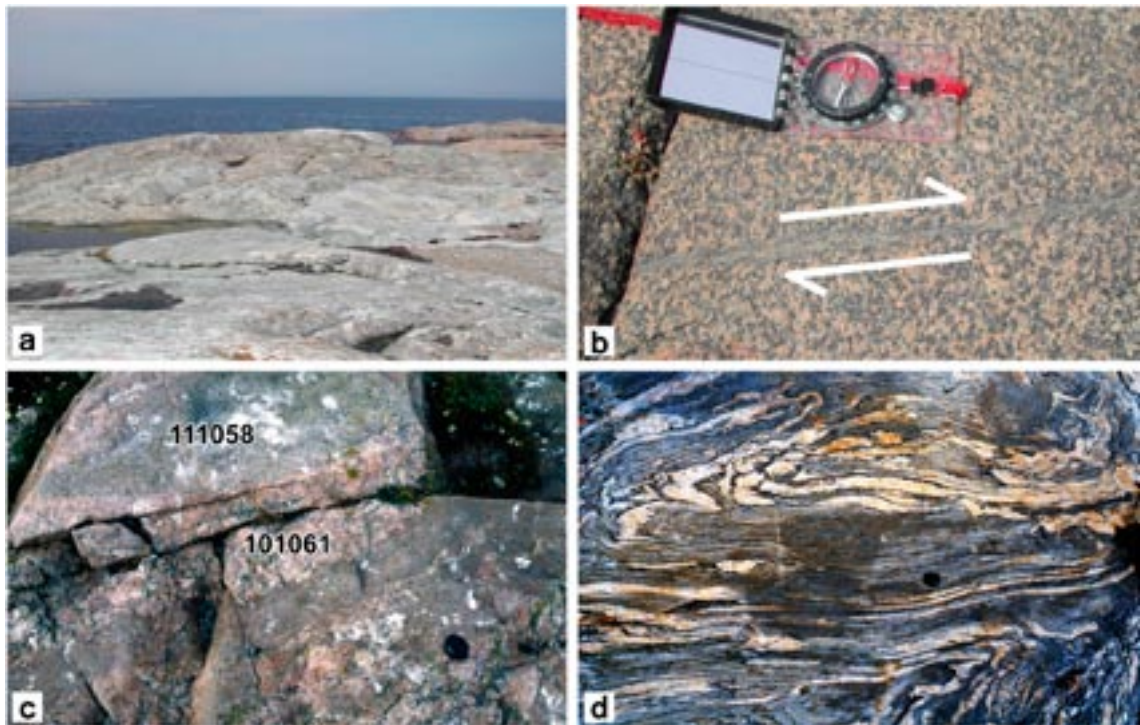


**Figure 5-14.** Field character of the rocks inside subarea 5 in the north-easternmost part of the area selected for mapping at Forsmark. a) General view of migmatitic meta-igneous rocks (migmatitic orthogneiss) on the island Norrkäret. b) Minor ductile shear zone with dextral strike-slip component of movement in Group B metadiorite that is generally not so much affected by ductile deformation (observation point PFM001068). c) Medium-grained granite with little ductile deformation (111058) intruded by pegmatite dykes (101061). All these rocks are inferred to belong to the Group D suite (observation point PFM005245). d) Folding of migmatitic veining in biotite-rich rock that is inferred to be supracrustal in origin and possibly a Group A metasedimentary rock (close to observation point PFM001676).

### **Ductile structures**

A linear grain-shape fabric is the principal ductile structure in the bedrock in subarea 5 and the bedrock is structurally dominated by LS-tectonites. The mineral stretching lineation plunges gently and shows a variable trend in the south-eastern quadrant on the stereographic projection plot (Figure 5-15). Minor fold axes plunge gently to the ESE (Figure 5-14d and Figure 5-15). The tectonic foliation is also variable in orientation with a dominant steep dip to the north-east and ENE (Figure 5-15). The younger granitic and pegmatitic dykes (Group D) generally show a steep orientation with variable dip direction (Figure 5-15). However, as in several other subareas, the dip direction is predominantly to the south and east, i.e. the poles to rock contacts plot mainly in the north-western quadrant on the stereographic projection plot (Figure 5-15).

### **Geophysical signature**

The north-easternmost part of the mapped area in subarea 5 is characterised by an irregular magnetic anomaly pattern of mostly moderate to low intensity (Figure 2-4 and /Isaksson et al. 2004a/). A local magnetic low correlates with the occurrence of the inferred Group D granite on the island Länsmän. For this reason, the magnetic anomaly map has been used to determine the distribution of this rock unit on the bedrock geological map. Since most of subarea 5 is covered by seawater, virtually no information can be obtained from the gamma-ray spectrometry data (Figure 2-6 and /Isaksson et al. 2004a/). The Bouguer gravity anomaly map (Figure 2-7) indicates a gentle gradient towards the north-east. However, the gravity stations are few and the knowledge of the gravity field distribution is poor.

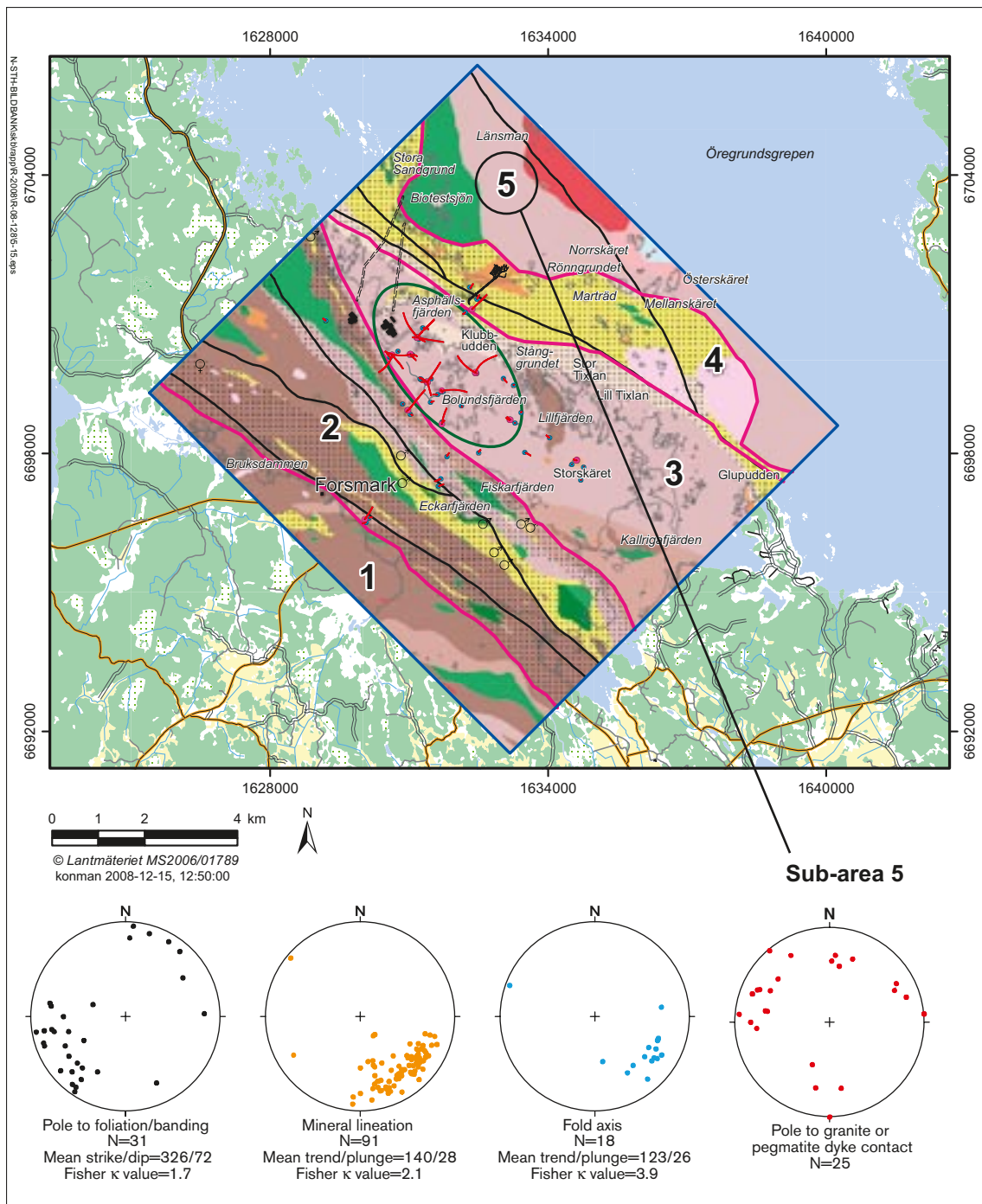


**Figure 5-15.** Orientation of ductile structures and Group D granitic and pegmatitic dykes at the ground surface in subarea 5. All structures and rock contacts have been plotted on the lower hemisphere of a Schmidt, equal-area stereographic projection. Planar structures and rock contacts have been plotted as poles to planes. The stereographic projections for the ductile structures are taken from /Stephens et al. 2003b/. The base map is the bedrock geological map of the area (see Figure 4-1 for legend).

### 5.3 Summary

An older suite of metagranitoids, included in the Group B rocks, strongly dominates the Forsmark area. Metatonalite and metagranodiorite are prominent in subareas 1 and 2 to the south-west of the candidate and target areas. Furthermore, larger bodies of metamorphosed quartz diorite to gabbro and ultramafic rocks, which are also included in the Group B suite, are conspicuous in these two subareas as well as in subarea 4. By contrast, Group B rocks with a granitic composition dominate inside the parts of the mapped area occupied by the candidate and target areas in subarea 3 and they are also inferred to dominate inside subarea 5. Group A felsic to intermediate metavolcanic rocks are prominent in subareas 2 and 4, while Group A rocks more confidently interpreted as sedimentary in origin are only present in the north-easternmost part of the mapped area in subarea 5. The distribution of these different rock types on the bedrock geological map is consistent with the pattern on the Bouguer gravity anomaly map (see also /Isaksson and Stephens 2007/).

All the rocks in Groups A and B show penetrative ductile deformation that occurred under amphibolite-facies metamorphic conditions; migmatitic rocks are present in the north-easternmost part of the mapped area in subarea 5. The ductile deformation in these rocks is expressed by the development of planar and linear grain-shape fabrics and, occasionally, by the development of a tectonic banding. Both the planar grain-shape fabric and tectonic banding in these rocks are commonly folded. Amphibolite occurs as enclaves within the tonalitic to granodioritic rocks and as disrupted dyke-like bodies and irregular inclusions in the granitic rocks. The amphibolites also show penetrative ductile deformation and are folded.

A predominantly fine- to medium-grained and younger suite of metagranitoids (Groups C and D) occurs as lenses, boudins and dykes in the older rocks. They are strongly subordinate to the rocks in Groups A and B and larger mappable rock units are restricted to subarea 4 to the east of the candidate and target areas. Granodioritic and tonalitic rocks dominate Group C, whereas granite, aplite, pegmatitic granite and pegmatite comprise Group D. Although there are different generations of pegmatite, which show different degrees of deformation and locally cross-cutting relations with respect to each other, all pegmatites in the area have been included in Group D.

The rocks in Groups C and D were affected by variable but generally a lower degree of ductile deformation compared with the older Group A and Group B rocks. In contrast to the older Group B rocks that show a tectonic banding and an intense foliation in high-strain belts, the Group C rocks in these belts occur as weakly discordant lenses or boudins with a simple, linear grain-shape fabric. Moreover, they do not contain the disrupted dyke-like bodies of amphibolite that are commonly present in the Group B rocks. The Group D rocks occur as dykes and minor bodies that commonly cross-cut the earlier ductile structures at high angles. They do not show the intensity of ductile strain described above in the Group C rocks. The field relationships suggest that the Group C rocks intruded during a late stage of the penetrative ductile deformation, which subsequently was completed prior to intrusion of the Group D granites. However, the Group D rocks are affected by combined ductile and brittle deformation along retrograde deformation zones.

The style and intensity of ductile strain at the Forsmark site is highly variable. High-strain belts with a WNW-ESE to NW-SE trend, which are prominent inside subareas 2 and 4, wrap around tectonic lenses with an apparently lower degree of ductile strain. Subarea 3 forms the most prominent tectonic lens (Forsmark tectonic lens). This variation is also reflected in the pattern on the magnetic anomaly map.

The bedrock in the high-strain belts shows a tectonic banding and both planar and linear grain-shape fabrics, i.e. they are SL-tectonites. The tectonic banding and foliation show the same orientation, with generally steep dips to the south-west. The linear grain-shape fabric plunges moderately or gently to the south-east. Intense, penetrative deformation under amphibolite-facies conditions as well as retrograde deformation, which is more spatially restricted, characterise these belts. Tubular-shaped folding is present on an outcrop scale in the highly deformed rocks to the north-east of the candidate area in subarea 4.

The tectonic lenses show a contrasting structural character. LS-tectonites, major folding and a generally lower degree of ductile deformation are present. On a mesoscopic scale, the folding deforms a tectonic foliation. Close to the nuclear power plant in subarea 3, the hinge of a major tubular fold structure is exposed within the most prominent tectonic lens at Forsmark. The fold axis plunges moderately towards the south-east, parallel to the linear grain-shape fabric. The fold also deforms a lithologically heterogeneous unit of predominantly fine-grained, felsic, meta-igneous rocks that show high ductile strain. The boundaries between rock units and the tectonic foliation in the rocks are parallel and all these planar structures are folded.



## 6 Uncertainties

No attempt has been made to quantify the uncertainty in the position of the boundaries between rock units on the bedrock geological map. As pointed out in chapter 4, these boundaries are based on a complex interplay between the frequency and quality of outcrop data and the character of the magnetic anomaly maps. In this context, it is important to keep in mind the variable resolution of the magnetic data (Figure 6-1). Furthermore, even in areas where the frequency of outcrops is strongly reduced, there can be a low uncertainty in the position of the boundaries between rock units if, for example, the magnetic data yield a highly variable pattern that can be confidently linked to different rock units in the areas where the frequency of outcrops is greater. Finally, the intrinsic complexity of the geology, as inferred from earlier investigations, is also an essential ingredient that bears an influence on the assessment of uncertainty. Simpler geology provides a better foundation for a lower degree of uncertainty.

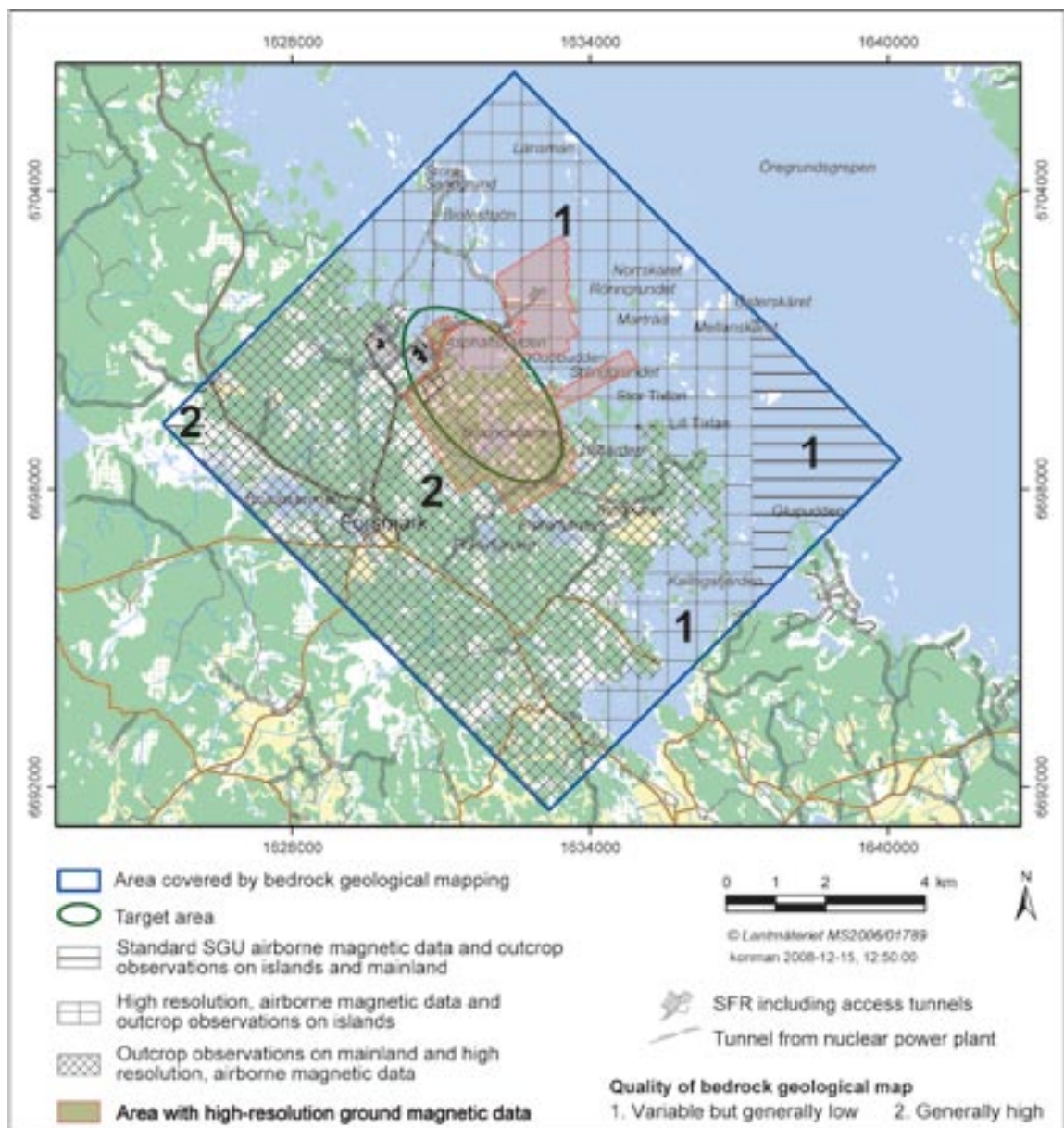


**Figure 6-1.** Frequency of outcrop, character of airborne magnetic data and qualitative judgement of the quality of the bedrock geological map.

On the basis of the considerations presented above, a qualitative judgement on the quality of the bedrock map and, as a consequence, the uncertainty in the position of boundaries between rock units has been made (Figure 6-1). This judgement is expressed in the form of two statements on the quality of the map – variable but generally low and generally high (Figure 6-1). Areas of the map where the quality of the bedrock map is variable but generally low are present in the north-eastern and south-eastern parts of the mapped area, i.e. in the archipelago (Figure 6-1). These areas are mainly covered by seawater. Areas where the quality of the bedrock map is generally high occur on the mainland (Figure 6-1).

## 7 References

- Aaro S, 2003.** Forsmark site investigation. Regional gravity survey in the Forsmark area, 2002 and 2003. SKB P-03-42, Svensk Kärnbränslehantering AB.
- Bergman T, Isaksson H, Johansson R, Lindèn A H, Lindroos H, Rudmark L, Stephens M, 1999.** Förstudie Tierp. Jordarter, bergarter och deformationszoner. SKB R-99-53, Svensk Kärnbränslehantering AB.
- Bergman T, Andersson J, Hermansson T, Zetterström Evins L, Petersson J, Albrecht L, Nordman C, Stephens M B, 2004.** Bedrock mapping. Stage 2 (2003) Bedrock data from outcrops and the basal parts of trenches and shallow boreholes through the Quaternary cover. Forsmark site investigation. SKB P-04-91, Svensk Kärnbränslehantering AB.
- Carlsten S, Gustafsson J, Petersson J, Samuelsson E, Stephens M B, Thunehed H, 2007.** Geological single-hole interpretation of KFM12A, HFM36 and HFM37. Forsmark site investigation. SKB P-07-110, Svensk Kärnbränslehantering AB.
- Cobbold P R, Quinquis H, 1980.** Development of sheath folds in shear zones. *Journal of Structural Geology* 2.
- Cronquist T, Forssberg O, Hansen L M, Jonsson A, Koyi S, Leiner P, Vestgård J, Petersson J, Skogsmo G, 2005.** Detailed fracture mapping of two trenches at Forsmark. Forsmark site investigation. SKB P-04-88, Svensk Kärnbränslehantering AB.
- Forssberg O, Hansen L M, Koyi S, Vestgård J, Öhman J, Petersson J, Albrecht J, Hedenström A, Gustavsson J, 2007.** Detailed fracture and bedrock mapping, Quaternary investigations and GPR measurements at excavated outcrop AFM001264. Forsmark site investigation. SKB P-05-269, Svensk Kärnbränslehantering AB.
- Hermanson J, Hansen L, Olofsson J, Sävås J, Vestgård J, 2003a.** Detailed fracture mapping at the KFM02 and KFM03 drill sites, Forsmark. SKB P-03-12, Svensk Kärnbränslehantering AB.
- Hermanson J, Hansen L, Vestgård J, Leiner P, 2003b.** Detailed fracture mapping of the outcrops Klubbudden, AFM001098 and drill site 4, AFM001097. Forsmark site investigation. SKB P-03-115, Svensk Kärnbränslehantering AB.
- Hermanson J, Hansen L, Vestgård J, Leiner P, 2004.** Detailed fracture mapping of excavated rock outcrop at drilling site 5, AFM100201. Forsmark site investigation. SKB P-04-90, Svensk Kärnbränslehantering AB.
- Isaksson H, Thunehed H, Keisu M, 2004a.** Interpretation of airborne geophysics and integration with topography. Stage 1 (2002). Forsmark site investigation. SKB P-04-29, Svensk Kärnbränslehantering AB.
- Isaksson H, Mattsson H, Thunehed H, Keisu M, 2004b.** Interpretation of petrophysical surface data. Stage 1 (2002). Forsmark site investigation. SKB P-03-102, Svensk Kärnbränslehantering AB.
- Isaksson H, Stephens M B, 2007.** Assessment of the validity of the rock domain model, version 1.2, based on the modelling of gravity and petrophysical data. Forsmark site investigation. SKB R-07-67, Svensk Kärnbränslehantering AB.
- Isaksson H, Thunehed H, Pitkänen T, Keisu M, 2007.** Detailed ground magnetic survey and lineament interpretation in the Forsmark area, 2006-2007. Forsmark site investigation. SKB R-07-62, Svensk Kärnbränslehantering AB.

- Koistinen T, Stephens M B, Bogatchev V, Nordgulen O, Wennerström M, Korhonen J, 2001.** Geological map of the Fennoscandian Shield, scale 1:2 000 000. Geological Surveys of Finland, Norway and Sweden and the North-West Department of Natural Resources of Russia.
- Leijon B (ed.), 2005.** Investigations of superficial fracturing and block displacements at drill site 5. Forsmark site investigation. SKB P-05-199, Svensk Kärnbränslehantering AB.
- Lindroos H, Isaksson H, Thunehed H, 2004.** The potential for ore and industrial minerals in the Forsmark area. SKB R-04-18, Svensk Kärnbränslehantering AB.
- Lundström I, 1995.** Beskrivning till berggrundskartorna Filipstad SO och NO. SGU Af 177, 185, Sveriges geologiska undersökning.
- Nilsson B, 2003.** Element distribution in till at Forsmark – a geochemical study. Forsmark site investigation. SKB P-03-118, Svensk Kärnbränslehantering AB.
- Passchier C W, Trouw R A J, 1998.** Microtectonics. Springer-Verlag, Berlin, Heidelberg.
- Petersson J, Berglund J, Danielsson P, Skogsmo G, 2005.** Petrographic and geochemical characteristics of bedrock samples from boreholes KFM04A–06A, and a whitened alteration rock. Forsmark site investigation. SKB P-05-156, Svensk Kärnbränslehantering AB.
- Petersson J, Skogsmo G, Vestgård J, Albrecht J, Hedenström A, Gustavsson J, 2007a.** Bedrock mapping and magnetic susceptibility measurements, Quaternary investigations and GPR measurements in trench AFM001265. Forsmark site investigation. SKB P-06-136, Svensk Kärnbränslehantering AB.
- Petersson J, Andersson U B, Berglund J, 2007b.** Scan line fracture mapping and magnetic susceptibility measurements across two low magnetic lineaments with NNE and NE trend, Forsmark. In Stephens M B and Skagius K (ed.), Geology – background complementary studies. Forsmark modelling stage 2.2. SKB R-07-56, Svensk Kärnbränslehantering AB.
- Rønning H J S, Kihle O, Mogaard J O, Walker P, Shomali H, Hagthorpe P, Byström S, Lindberg H, Thunehed H, 2003.** Helicopter borne geophysics, Östhammar, Sweden. Forsmark site investigation. SKB P-03-41, Svensk Kärnbränslehantering AB.
- SKB, 2000.** Samlad redovisning av metod, platsval och program inför platsundersökningskedet (Fud-k). Svensk Kärnbränslehantering AB.
- SKB, 2004.** Preliminary site description Forsmark area – version 1.1. SKB R-04-15, Svensk Kärnbränslehantering AB.
- SKB, 2005a.** Programme for further investigations of geosphere and biosphere. Forsmark site investigation. SKB R-05-14, Svensk Kärnbränslehantering AB.
- SKB, 2005b.** Preliminary site description Forsmark area – version 1.2. SKB R-05-18, Svensk Kärnbränslehantering AB.
- SKB, 2006.** Site descriptive modelling Forsmark stage 2.1. Feedback for completion of the site investigation including input from safety assessment and repository engineering. SKB R-06-38, Svensk Kärnbränslehantering AB.
- Sohlenius G, Hedenström A, Rudmark L, 2004.** Mapping of unconsolidated Quaternary deposits 2002–2003. Map description. SKB R-04-39, Svensk Kärnbränslehantering AB.
- Stephens M B, Bergman T, Andersson J, Hermansson T, Wahlgren C-H, Albrecht L, Mikko H, 2003a.** Bedrock mapping. Stage 1 (2002) – Outcrop data including fracture data. Forsmark site investigation. SKB P-03-09, Svensk Kärnbränslehantering AB.

**Stephens M B, Lundqvist S, Bergman T, Anderson J, Ekström M, 2003b.** Forsmark site investigation. Bedrock mapping. Rock types, their petrographic and geochemical characteristics, and a structural analysis of the bedrock based on Stage 1 (2002) surface data. SKB P-03-75, Svensk Kärnbränslehantering AB.

**Stephens M B, Lundqvist S, Bergman T, Ekström M, 2005.** Forsmark site investigation. Bedrock mapping. Petrographic and geochemical characteristics of rock types based on Stage 1 (2002) and Stage 2 (2003) surface data. SKB P-04-87, Svensk Kärnbränslehantering AB.

**Stephens M B, Fox A, La Pointe P, Simeonov A, Isaksson H, Hermanson J, Öhman J, 2007.** Geology Forsmark. Site descriptive modelling Forsmark stage 2.2. SKB R-07-45, Svensk Kärnbränslehantering AB.

**Stephens M B, Simeonov A, Isaksson H, 2008.** Bedrock geology Forsmark, Modelling stage 2.3. Implications for and verification of deterministic geological models based on complementary data. SKB R-08-64, Svensk Kärnbränslehantering AB.

**Stålhös G, 1991.** Beskrivning till berggrundskartorna Östhammar NV, NO, SV, SO. SGU Af 161, 166, 169, 172, Sveriges geologiska undersökning.

**Söderbäck B (ed.), 2008.** Geological evolution, palaeoclimate and historical development of the Forsmark and Laxemar-Simpevarp areas. Site descriptive modelling, SDM-Site. SKB R-08-19, Svensk Kärnbränslehantering AB.

## Coding of rock type along cored boreholes drilled during the construction of the Forsmark nuclear power plant and SFR

### Introduction

This appendix provides a summary of a study that was initiated to convert the information on rock types from cored boreholes, drilled during construction of the Forsmark nuclear power plant and the SFR facility, to the rock nomenclature used within the Forsmark site investigation programme. The principal objective of this study was to enable correlation with the cored borehole and surface mapping data carried out during the site investigation programme.

An inventory to retrieve and structure available data from the boreholes was initially provided by /Keisu and Isaksson 2004/. During this work, all boreholes were assigned a new identity code and all the geological logs available from the drilling campaigns in connection with the feasibility study and construction of the Forsmark nuclear power plant were digitized. No such digitization was carried out for the drill cores close to the SFR facility. At the time of the investigation, a few drill cores were stored in SKB's archive near Uppsala, while most drill cores were available for study at the Geological Survey of Sweden's (SGU) archive at Malå, Västerbotten, in northern Sweden. However, material from parts of several drill cores was missing in these archives. The material stored in Malå consisted of 41 drill cores from the construction of the Forsmark nuclear power plant (identity code KFK) and 42 drill cores from the SFR facility (identity code KFR). Only drill cores with a geological log were of interest for the rock coding study. This restricted the amount of relevant drill cores to 32 with identity code KFK and 27 with identity code KFR (Table A-1).

**Table A-1. KFK and KFR drill cores along which rock types have been coded for rock type following core inspection.**

New ID code	Old ID code	Drill site	Boxes in Malå (length)	Mapped by	Comment
KFK003	DBT 3	Reactor site 3	13,14 (45.85–54 m), 17 (c. 61–65 m)	Bergman/Stephens	
KFK037	D354	Reactor site 3	1–5 (0.00–31.10 m)	Bergman/Stephens	
KFK040	D357	Reactor site 3	1–7 (0.00–45.91 m)	Bergman/Stephens	
KFK041	D358		1–9 (0.00–31.65 m)	Bergman/Stephens	
KFK044	D361	Reactor site 3	2–8 (0.00–44.05 m)	Petersson/Skogsmo	
KFK049	D366	Reactor site 3	1–6 (0.00–34.80 m)	Bergman/Stephens	Strongly banded and heterogeneous at 1.08–2.25 m.
KFK058	D381	Tunnel from reactor site 3	1–22 (17.30–174.52 m)	Bergman/Stephens	Porphyritic at 50.65–52.73 m (also multiple fracture filling). Skarn-related hematite mineralisation at 64.73–64.78 m.
KFK059	D382	Tunnel from reactor site 3	1–23 (19.00–172.93 m)	Petersson/Skogsmo	Mica-altered at 60.48–65.60 m. Chlorite + hematite/epidote alteration at 101.40–112.18, 113.36–114.88, 134.40–142.40 and 148.72–172.93 m.
KFK060	D383	Tunnel from reactor site 3	1–24 (15.85–170.00 m)	Bergman/Stephens	All felsic to intermediate metavolcanic rocks are mica-altered.
KFK061	D392		1–23 (0.00–149.77 m)	Bergman/Stephens	
KFK062	D395		1–24 (0.00–136.07 m)	Bergman/Stephens	K-Na-altered (?) metagranite-granodiorite (101057) at 33.10–33.56 m.
KFK063	DR3-1	Reactor site 3	1–4 (0.00–20.61 m)	Bergman/Stephens	
KFK064	DR3-2	Reactor site 3	1–3 (0.00–29.91 m)	Bergman/Stephens	
KFK066	DR3-4	Reactor site 3	2–4 (0.00–20.44 m)	Bergman/Stephens	Vuggy granite (i.e. episyenite) at 10.90–15.25 m.

New ID code	Old ID code	Drill site	Boxes in Malå (length)	Mapped by	Comment
KFK068	DR3-6	Reactor site 3	1–2 (0.00–15.16 m)	Petersson/Skogsmo	
KFK074	D41	Reactor site 1 and 2	1–4 (0.00–32.60 m)	Petersson/Skogsmo	
KFK075	D42	Reactor site 1 and 2	2–3 (0.73–30.17 m)	Petersson/Skogsmo	Pegmatitic granite at 0.73–6.60 m, proceeds down to 11.40 m.
KFK076	D43	Reactor site 1 and 2	1–4 (0.00–35.10 m)	Bergman/Stephens	Hydrothermally altered with biotite flecks. Essentially metagranite (101057).
KFK077	D44	Reactor site 1 and 2	1–4 (0.00–35.00 m)	Bergman/Stephens	Hydrothermally altered with biotite flecks. Essentially metagranite (101057).
KFK079	D62	Tunnel from reactor site 1 and 2	1 (0.00–9.02 m)	Petersson/Skogsmo	
KFK080	D62A	Tunnel from reactor site 1 and 2	1–8 (0.00–79.30 m)	Bergman/Stephens	
KFK081	D63	Tunnel from reactor site 1 and 2	2–9 (23.50–85.00 m)	Bergman/Stephens	
KFK083	D65	Tunnel from reactor site 1 and 2	1–24 (19.15–163.40 m)	Bergman/Stephens	All felsic to intermediate metavolcanic rocks are mica-altered. Critical boundary at 63.60 m.
KFK084	D66	Tunnel from reactor site 1 and 2	1–22 (17.40–157.30 m)	Bergman/Stephens	Deformation zone beneath 78.33 m.
KFK085	D67	Tunnel from reactor site 1 and 2	1 (14.55–20.10 m), 3–13 (25.80–95.87 m)	Petersson/Skogsmo	
KFK087	D71	Reactor site 1 and 2	1–3 (0.00–25.50 m)	Bergman/Stephens	Hydrothermally altered with biotite flecks. Also some 111058; not separated from 101057.
KFK088	D72	Reactor site 1 and 2	1–2 (0.00–19.24 m)	Bergman/Stephens	
KFK116	D4	Reactor site 1 and 2	1–7 (4.30–59.95 m)	Bergman/Stephens	Hydrothermally altered with biotite flecks down to 48.3 m. Similar to that in KFM076–77 and KFK087. Also some 101051 (granodioritic) at 51.3–51.8 m.
KFK117	D5	Reactor site 1 and 2	1–5 (0.00–42.00 m)	Bergman/Stephens	Some 111058 at 5.00–6.51 m. Altered metagranite (101057) with biotite flecks at c. 9 m.
KFK118	D6	Reactor site 1 and 2	1–7 (4.80–60.40 m)	Bergman/Stephens	
KFK119	D8	Reactor site 1 and 2	1–7 (3.90–58.30 m)	Bergman/Stephens	
KFK120	D11	Reactor site 1 and 2	1–5 (3.30–40.20 m)	Bergman/Stephens	
KFR02	HK3	SFR	1–19 (0.00–99.25 m)	Bergman/Stephens	Zone H2(?) at 84.28–94.17 m.
KFR03	HK4	SFR	1–18 (0.00–100.50 m)	Petersson/Skogsmo	
KFR04	HK5	SFR	1–7 (0.60–131.40 m)	Petersson/Skogsmo	Oxidation of 103076 at 63.00–75.90, 84.93–88.75, 104.16–105.05 and 106.92–120.30 m.
KFR7B	HK7B	SFR	1–4 (0.00–21.10 m)	Petersson/Skogsmo	Fine-grained variety of 101057 at 13.00–16.20 and 16.95–21.10 m.
KFR7C	HK7C	SFR	1–6 (0.00–34.00 m)	Petersson/Skogsmo	Fine-grained variety of 101057(?), or possibly a rhyolitic, more coarse-grained variety of 103076 from 14.41 to the bottom of the drill core.

New ID code	Old ID code	Drill site	Boxes in Malå (length)	Mapped by	Comment
KFR08	HK8	SFR	1–19 (0.00–104.04 m)	Petersson/Skogsmo	Ductile deformation zone at 41.59–46.00 m, brittle-ductile deformation zone at 46.00–49.77 and 51.00–74.90 m. Zone 8(?). Strongly oxidized 103076 at 774.90–104.40 m. Vuggy granite (i.e. episyenite) at 72.69–73.23 m.
KFR09	HK9	SFR	1–14 (0.00–80.29 m)	Petersson/Skogsmo	Oxidation of 103076 at 3.44–22.65 and 24.40–59.25 m.
KFR10	HK10	SFR	1–20 (0.00–103 m)	Petersson/Skogsmo	
KFR11	HK11	SFR	1–18 (0.00–97.81 m)	Bergman/Stephens	Penetratively deformed metatonalite-granodiorite (101054) at 18.73–32.35 m. Slightly coarser K-feldspar in a fine-grained matrix – high level intrusion? Zone 8 from 62.44 to the bottom of the drill core. Difficult to recognize type of granite in the deformation zone; possibly 111058. Vuggy granite at 73.02–73.30 and 92.01–92.15 m.
KFR12	HK12	SFR	1–9 (0.00–50.26 m)	Bergman/Stephens	Fine-grained, greyish red, penetratively foliated variety of 101057(?) at 16.19–36 m.
KFR13	HK13	SFR	1–14 (0.00–76.60 m)	Petersson/Skogsmo	Possibly fine-grained variety of 101057 instead of 103076 at 36.54–38.90 and 40.20–42.16 m. Oxidized 103076 at 21.13–22.19 m.
KFR14	HK14	SFR	2–6 (5.50–28.67 m)	Petersson/Skogsmo	
KFR19	KB19	SFR	1–20 (0.00–110.17 m)	Petersson/Skogsmo	
KFR20	KB20	SFR	1–20 (0.00–108.76 m)	Petersson/Skogsmo	Fine-grained, greyish red, penetratively foliated variety of 101057(?) at 0–4.60 and 5.70–23.80 m, and locally at 61.60–88.10 m.
KFR52	KB22	SFR	1–11 (0.00–29.95 m)	Petersson/Skogsmo	
KFR54	KB24	SFR	1–10 (0.00–53.30 m)	Petersson/Skogsmo	101057 typically oxidized at 28.65–39.45 m
KFR55	KB25	SFR	1–11 (0.00–61.90 m)	Petersson/Skogsmo	Possibly fine-grained variety of 101057 instead of 103076 at 39.03–45.80 m.
KFR57	KB27	SFR	1–5 (0.00–23.48 m)	Petersson/Skogsmo	Uncertain if the rock type should be coded as 103076 or as a fine-grained variety of 101057 in the interval 4.58–15.93 m.
KFR61	DS1	SFR	1–13 (1.43–70.90 m)	Bergman/Stephens	Singö deformation zone from 51.21 m to the bottom of the drill core.
KFR62	DS2	SFR	1–15 (1.40–82.20 m)	Petersson/Skogsmo	Brittle-ductile deformation zone from 62.87 m to the bottom of the drill core. Probably Singö zone.
KFR63	DS3	SFR	1–4 (0.00–15.08 m)	Petersson/Skogsmo	
KFR64	DS4	SFR	1–9 (0.00–41.38 m)	Petersson/Skogsmo	Brittle-ductile deformation zone at 2.04–7.00 and 13.10–40.5(?). Probably Singö zone. Mica-altered 103076(?) at 30.76–34.10 and 36.00–40.35 m.
KFR65	DS5	SFR	1–6 (0.00–28.95 m)	Petersson/Skogsmo	
KFR66	DS6	SFR	1–4 (0.00–14.18 m)	Petersson/Skogsmo	Major brittle deformation zone. Strongly altered and not always possible to recognize the protolith. Singö zone?
KFR67	DS7	SFR	1–5 (0.00–35.21 m)	Petersson/Skogsmo	
KFR68	DS8	SFR	1–21 (0.00–115.80 m)	Petersson/Skogsmo	Fine-grained variety of 101057(?) at 0.0–18.90 m.
	SFR (SILO1)	SFR	1–16 (0.00–45.12 m)	Petersson/Skogsmo	Seems to be both 103076 and a fine-grained variety of 101057(?). Difficult to separate the two rocks. Ductile deformation zone at 11.06–11.09 m.



## Execution

Based on the descriptive text written in the geological logs, a translation into the SKB rock code system was initially completed by SKB for the KFK drill cores, without any inspection of these drill cores. Subsequently, 25 of the KFK boreholes and four of the KFR boreholes were inspected at Malå by Torbjörn Bergman and Michael Stephens (SGU) during April 2004 (Table A-1) and new rock codes were assigned to the rock type identified in the original geological log. The remaining 30 boreholes were inspected and coded by Jesper Petersson and Göran Skogsmo (SwedPower AB) during August 2004 (Table A-1). In order to store the data from this activity according to the structure in SKB's database Sicada, it was also necessary to digitize the old geological logs from the drill cores with KFR identity. This was carried out by Göran Skogsmo (SwedPower AB).

Irrespective of borehole length, all rock units recorded in the original geological logs were provided with a rock code according to the nomenclature used within the site investigation programme. The digitized geological logs are condensed versions of the original logs, which are normally more detailed, and may include information regarding fracture intensity and geophysical properties. It is important to emphasise that none of these data were modified during the rock coding study. Complementary information from the inspection work carried out in the context of this study, including observations on structure, alteration and other significant features, are provided in Table A-1. These observations have not been included in SKB's Sicada database.

## Results

The initial translated rock codes in the KFK drill cores and the new rock codes determined after inspection of both the KFK and KFR drill cores have been archived in the Sicada database. In general, the lithology along the drill cores from the construction of the Forsmark nuclear power plant corresponds well with what might be expected from the surface bedrock mapping in the area /Stephens et al. 2003/. The dominant rock type in the area around reactor site 1 and 2 is the medium-grained metagranite-granodiorite (rock code 101057) that is prominent inside the candidate area at Forsmark /e.g. SKB 2004/. Amphibolite (rock code 102017) and pegmatitic granite (rock code 101061) form subordinate rock types. A significant feature in boreholes KFK076, KFK077, KFK087, KFK116 and KFK117 is a bleached, hydrothermally altered rock with biotite aggregates (see Figure 5-8e in section 5.2.3 in the main text). This alteration is pre- or possibly syn-metamorphic in character triggered by heat from younger intrusions /Petersson et al. 2005, Stephens et al. 2007/.

At reactor site 3, the main rock type contains a lower content of K-feldspar and the dominant rock varies from medium-grained metagranite-granodiorite (rock code 101057) to metagranodiorite (rock code 101056) and metatonalite-granodiorite (rock code 101054). Amphibolite and pegmatitic granite occur subordinately. Occurrences of aplitic metagranite (rock code 101058) have also been recorded in boreholes KFK044 and KFK049.

The majority of the drill cores from the areas close to the tunnels from reactor site 1 and 2 and reactor site 3 are dominated by felsic to intermediate metavolcanic rock (rock code 103076). Some intervals of this rock show a variable degree of mica alteration. A critical boundary occurs at 63.6 m depth in KFK083. The dominant rock type south-west of this boundary (i.e. in KFK081, KFK084 and the lower 100 m of KFK083) is an aplitic metagranite (rock code 101058) that is commonly highly deformed. Pegmatitic granite and amphibolite occur subordinately in all the tunnel drill cores.

The dominant lithology in the drill cores from the construction of SFR is generally similar to that in the KFK drill cores. However, the proportions between different lithologies are somewhat different. The dominant rock types include a red, fine- to finely medium-grained, equigranular granite (rock code 111058), felsic to intermediate metavolcanic rock (rock code 103076) and a fine- to finely medium-grained variety of metagranite-granodiorite (rock code 101057). The latter is often difficult to separate from the metavolcanic rock, especially in more fine-grained intervals (for example in KFR7C, KFR13, KFR55 and KFR57). Other constituents

of less volumetric importance are pegmatitic granite and amphibolite. The series of drill cores located adjacent to or inside the Singö deformation zone (i.e. KFR61–67) are all composed of felsic to intermediate metavolcanic rock and pegmatitic granite, with minor amounts of amphibolite. In addition to the drill cores associated with the Singö deformation zone, there are three drill cores that penetrate significant deformation zones: KFR02 84.3–94.2 m, KFR08 41.6–74.9 m and KFR11 62.4–97.8 m.

## References

**Keisu M, Isaksson H, 2004.** Forsmark site investigation. Acquisition of geological information from Forsmarksverket. Information from the Vattenfall archive, Räcksta. SKB P-04-81, Svensk Kärnbränslehantering AB.

**Petersson J, Berglund J, Danielsson P, Skogsmo G, 2005.** Petrographic and geochemical characteristics of bedrock samples from boreholes KFM04A–06A, and a whitened alteration rock. Forsmark site investigation. SKB P-05-156, Svensk Kärnbränslehantering AB.

**SKB, 2004.** Preliminary site description. Forsmark area – version 1.1. SKB R-04-15, Svensk Kärnbränslehantering AB.

**Stephens M B, Bergman T, Andersson J, Hermansson T, Wahlgren C-H, Albrecht L, Mikko H, 2003.** Bedrock mapping. Stage 1 (2002) – Outcrop data including fracture data. Forsmark site investigation. SKB P-03-09, Svensk Kärnbränslehantering AB.

**Stephens M B, Fox A, La Pointe P, Simeonov A, Isaksson H, Hermanson J, Öhman J, 2007.** Geology Forsmark. Site descriptive modelling Forsmark stage 2.2. SKB R-07-45, Svensk Kärnbränslehantering AB.